

1 **A large panel of chicken cells are invaded *in vivo* by *Salmonella***

2 **Typhimurium even when depleted of all known invasion factors**

3 S. M. Roche^{1,2}, S. Holbert^{1,2}, Y. Le Vern^{1,2}, C. Rossignol^{1,2}, A. Rossignol^{1,3}, P. Velge^{1,2} and
4 I. Virlogeux-Payant^{1,2*}

5 ¹*INRAE, UMR1282 Infectiologie et Santé Publique, F-37380 Nouzilly, France*

6 ²*Université François Rabelais de Tours, UMR1282 Infectiologie et Santé Publique, F-37000*
7 *Tours, France*

8 ³*present address: Lycée Grandmont - Laboratoire de Biotechnologies, F-37204, TOURS,*
9 *France*

10

11 *For correspondence email

12 isabelle.virlogeux-payant@inrae.fr

13

14 **Short title:** *In vivo* cellular invasion of *S. Typhimurium* in chicks

15

16 **Abstract**

17 *Salmonella* are among the most important foodborne pathogens and contaminated
18 poultry meat and eggs are the main source of human infection. Infected poultry are a major
19 problem as they are asymptomatic, thus rendering the identification of infected poultry farms
20 difficult. In this context, controlling animal infections is of primary importance. It is known that
21 cell and tissue tropism govern disease in many infectious models, our aim was therefore to
22 identify the infected host-cell types in chicks and the role of the three known bacterial invasion
23 factors in this process (T3SS-1, Rck and PagN). Chicks were inoculated with wild-type or
24 isogenic fluorescent *Salmonella* Typhimurium mutant strains via the intraperitoneal route. Then
25 infected cells in the liver, spleen, gall bladder and aortic vessels were identified using flow-
26 cytometric analyses and invasion confirmed by confocal microscopy. Our results show that all
27 these organs could be *foci* of infection and that a wide array of phagocytic and non-phagocytic

28 cells is invaded *in vivo* in each organ. These cells include immune cells and also epithelial and
29 endothelial cells. Moreover, we demonstrated that, despite the invalidation of the three known
30 invasion factors (T3SS-1, Rck and PagN), *S. Typhimurium* remained able to colonize internal
31 organs and invade non-phagocytic cells in each organ studied. In line with this result, the mutant
32 strains colonized these organs more efficiently than the wild-type strain. *S. Typhimurium*
33 invasion of gall bladder cells was confirmed by immunohistochemistry and infection was
34 shown to last several weeks after inoculation of chicks and at a level similar to that observed in
35 the spleen. All together, these findings provide new insights into the dynamics of *Salmonella*
36 spread *in vivo* in chicks at the organ and cellular levels.

37

38 **Author summary**

39 In many infectious models, cell and tissue tropism govern disease. Moreover, depending
40 on the entry process, both bacterial behavior and host response are different. It is therefore
41 important to identify the host cells targeted *in vivo* by a pathogen and the entry routes used by
42 this pathogen to invade the different host cells. This is all the more important with a pathogen
43 that enters cells in several ways like *Salmonella*, which is responsible for human and animal
44 salmonellosis. As poultry meat and eggs are the main sources of human contamination,
45 controlling animal infections is of primary importance. In this paper, we identified a large array
46 of phagocytic and non-phagocytic cells targeted *in vivo* using fluorescent *Salmonella*
47 Typhimurium strains inoculated by the intraperitoneal route. Surprisingly, the same host cells
48 were infected by the wild-type strain or its isogenic mutants deleted of either the T3SS-1 or of
49 the three known invasion factors (T3SS-1, Rck and PagN). These cells were immune cells but
50 also epithelial and endothelial cells. Moreover, we demonstrated for the first time that the gall

51 bladder and the aortic vessels could be *foci* of infection in chicks in addition to the liver and
52 spleen.

53

54 **Introduction**

55 *Salmonella* spp. are among the most important foodborne pathogens. From a public
56 health perspective, according to the World Health Organization, *Salmonella* spp. are among the
57 31 diarrheal and/or invasive agents (viruses, bacteria, protozoa, helminths, and chemicals)
58 displaying the highest capability of triggering intestinal or systemic diseases in humans. Most
59 cases of salmonellosis are mild, but sometimes the disease is life-threatening and salmonellosis
60 is the third leading cause of death among food-transmitted diseases (1).

61 The two most commonly reported non-typhoidal serovars *Salmonella enterica* subsp.
62 *enterica* serovar Enteritidis and *Salmonella enterica* subsp. *enterica* serovar Typhimurium
63 (including its monophasic variant) accounted for almost 80% of human cases occurring in the
64 EU (2). Depending on host factors and serovars, *Salmonella* can induce a wide range of diseases
65 ranging from systemic to asymptomatic infections and gastroenteritis (3). In humans, localized
66 infections can be followed by bacteremia in 3 to 10% of cases (4).

67 Animals are the primary source of these pathogens and humans become infected mainly
68 by ingesting contaminated food. Poultry meat and eggs are the main source of human
69 *Salmonella* contamination. In 2010, Knight-Jones *et al.* reported that poultry was implicated as
70 an outbreak source in 10.4% of the total cases worldwide (5). Since 2018, it has remained the
71 highest prevalence of *Salmonella*-positive single samples from official control investigations
72 (2). The detection and eradication of *Salmonella* in poultry is difficult because *Salmonella*
73 mostly induce an asymptomatic infection, accompanied by high fecal excretion, which is a
74 source of transmission (6). This leads to contaminated poultry flocks that must therefore be

75 eradicated and all derived products destroyed, resulting in high economic losses. It is therefore
76 particularly important to control animal infection not only to avoid economic consequences but
77 also for the negative impacts for human health.

78 To establish infection in their hosts, *Salmonella* have to interact with several phagocytic
79 and non-phagocytic eukaryotic cells. Invasion of these cells is considered as one of the most
80 important steps in *Salmonella* pathogenesis. The most well-described invasion process requires
81 the Type III Secretion System – 1 (T3SS-1) encoded by *Salmonella* pathogenicity island 1 (SPI-
82 1). The T3SS-1 is a needle-like structure, which directly injects bacterial effector proteins into
83 the host cytosol to manipulate the cell cytoskeleton, allowing bacterial internalization into non-
84 phagocytic cells (7). Two other *in vitro* entry pathways, involving the Rck and PagN invasins,
85 have also been described in *Salmonella* (8-10). Contrary to the T3SS-1, each invasin interacts
86 with an eukaryotic receptor, EGFR and the heparinated proteoglycan for Rck and PagN,
87 respectively (11, 12). *In vivo*, several reports particularly in mice have shown the key role of
88 the T3SS-1 for *Salmonella* to cross the intestinal barrier (13, 14). Nevertheless, infections in
89 the absence of T3SS-1 in mice, chicks and calves have also been described in several papers in
90 which a mutant, defective for the T3SS-1, was shown to colonize its host as well as its wild-
91 type parent (15-20). This observation has also been made in humans in whom food-borne
92 disease outbreaks have been described with *Salmonella* Senftenberg isolates which lack
93 segments of SPI-1 (21). In the same way, a study performed by Suez *et al.* comparing the
94 pathogenicity of different non-typhoidal strains concluded that *Salmonella* virulence factors,
95 including multiple T3SS effectors, were absent from several bacteremia isolates suggesting
96 they are dispensable for invasive infection (22). Less is known about the role of the Rck and
97 PagN invasins *in vivo* but *pagN* (formerly *iviVI-A*) and *rck* mutants are both less competitive
98 than their wild-type parent in mice (23-25). However, apart from these roles identified at the

99 organ level, very little is known about the cells targeted by these invasion factors and this is
100 even more true in farm animals.

101 This topic is crucial because cell and tissue tropism governs disease in many models
102 (26, 27). Moreover, some studies have shown that depending on the entry mechanism both
103 bacterial behavior and host response are different (28). It is therefore important to identify the
104 host cells targeted by *Salmonella* and the different entry routes used by this pathogen to invade
105 the different host cells. In order to improve understanding of how *Salmonella* infect chicks, our
106 aim was to identify cells that could be targeted *in vivo* by this pathogen, expressing or not the
107 known invasion factors. For this purpose, we used a fluorescent *S. Typhimurium* wild-type
108 strain and its fluorescent mutant derivatives deleted of either the T3SS-1 alone or of the three
109 known invasion factors (T3SS-1, Rck and PagN) to infect chicks intraperitoneally. Among the
110 different organs, the spleen, liver and gall bladder were chosen to be potential foci of infection
111 (29). Moreover, vessels from the aortic arch with the brachiocephalic trunk called “aortic
112 vessels” in the article were also collected to analyze putative infection of endothelial cells. In
113 these organs and vessels, identification of phagocytic and non-phagocytic cells and their
114 invasion by the different bacteria were followed using flow cytometric analyses and confocal
115 microscopy.

116

117 **Results – Discussion**

118 *Mutant strains defective for the T3SS-1 or the three known invasion factors inoculated by the*
119 *intraperitoneal route, colonize chicks more effectively than their wild-type parent strain*

120 Previous work has shown that a $\Delta invA$ mutant strain (T3SS-1 defective strain) and a
121 strain deleted for the three known invasion factors (3Δ) remained invasive for several
122 eukaryotic cell lines compared to the wild-type strain (30). To determine the ability of our wild-
123 type strain and our mutant strains to invade *in vivo* several host cells, we chose to bypass the

124 intestinal barrier and to infect chicks by the intraperitoneal route. The first step was to evaluate
125 the ability of these different strains to colonize vessels and several organs of chicks i.e. the
126 spleen, liver and gall bladder (Fig 1). To ensure that the levels of bacteria were not related to
127 the presence of *Salmonella* in the blood, all chicks were bled.

128 The first observation is that all strains were able to infect all the organs and vessels. For
129 some animals, the infection rate even reached 8 log CFU/g, especially for the gall bladder.
130 Moreover, all organ colonization levels were higher after inoculation with the $\Delta invA$ strain
131 compared to that with the wild-type strain (29, 35, 3.9 and 12 times more in the spleen, liver,
132 aortic vessels, and gall bladder, respectively). All these differences were statistically significant.
133 While the 3Δ strain also colonized these organs and vessels, more effectively than the wild-
134 type strain (9.5, 13, 2.6 and 5.1 times more in the spleen, liver, aortic vessels, and gall bladder,
135 respectively), a statistically significant difference was only identified in the liver. No significant
136 statistical difference could be observed between the two mutants, beside the fact that the log
137 CFU of bacteria/g for the 3Δ strain was always inferior to that of bacteria/g of organ for the
138 $\Delta invA$ strain. The levels of CFU recovered in the gall bladder and the aortic vessels should be
139 highlighted, as they have previously been rarely studied. These results demonstrated that all the
140 tested organs and vessels are colonized by *S. Typhimurium* and that the two mutant strains
141 ($\Delta invA$ or 3Δ) colonized deep organs of chicks after intraperitoneal inoculation at least at the
142 same level as the wild-type strain.

143 This latter result could be attributed to the route of inoculation. Indeed, *Salmonella*
144 injected *via* the intraperitoneal route easily reaches systemic sites such as the spleen and the
145 liver. They could also reach the gall bladder through the vasculature or the hepatic duct (31). *In*
146 *vivo* studies have demonstrated that the T3SS-1 is primarily associated with the early stage of
147 infection in which it translocates T3SS1 effectors across the host intestinal epithelial cell
148 membrane and stimulates intestinal inflammation (13) (14, 32-34) and is therefore important

149 for *Salmonella* colonization after animals are inoculated orally. Our results show that, in
150 chicken, the colonization of deeper organs can be independent of this type III secretion system
151 as no difference in colonization between a T3SS-1 mutant and its wild-type parent was observed
152 as described after intraperitoneal or intravenous inoculation of mice. Several reports have also
153 suggested that *Salmonella* remain pathogenic without an active T3SS-1 even after oral
154 inoculation in several animal models, including chicks (19, 20, 35). Moreover, a *Salmonella*
155 Senftenberg strain lacking T3SS-1 was isolated from a human clinical case and has been shown
156 to be able to induce enterocolitis in a mouse model (21). In our case, one hypothesis that could
157 explain the higher colonization of the mutant strains compared to the wild-type strain is that,
158 after intraperitoneal inoculation, the absence of the T3SS-1 could induce a lower immune
159 system alert, especially a lower inflammatory response and consequently less killing of
160 bacterial. Indeed, SPI-1 genes are involved in the regulation of the host immune response, for
161 example the host inflammatory response (36), immune cell recruitment (37) and apoptosis (38,
162 39). Moreover, we already know that a SPI-1 mutant and also a *phoP* mutant, not expressing
163 PagN like our 3Δ mutant, did not stimulate an inflammatory response in the caecum of chicks
164 (40).

165

166 Cytometric analyzes and microscopy were then performed in order to determine whether
167 *Salmonella* was within the cells of the different organs and vessels and to identify the cell-types
168 infected. The infectious dose of 6.10^7 CFU/chick used for the previous *in vivo* experiment,
169 represented a good compromise between the infectious dose and the period of slaughter (2
170 days), in order to potentially detect enough intracellular bacteria for flow cytometry analyses.
171 The animals were bled to decrease red blood cells and allow better detection of organ cells. The
172 concentration of *S. Typhimurium*-TurboFP650-wild-type strain was checked in the blood of six
173 animals. An average of 1.95 ± 1.09 log CFU/mL was found.

174

175 *STM-Turbo FP650-WT and its mutant strains were within the cells and did not only adhered to*
176 *the cells*

177 As our aim was to identify cells infected by *Salmonella*, we first assessed whether our
178 protocol allowed us to identify intracellular bacteria or not. Indeed, flow cytometry is useful for
179 quantitative analyses but it does not allow the intracellular localization of bacteria to be
180 determined as adherent bacteria could exist. According to our protocol, it was highly unlikely
181 that *Salmonella* would only be present extracellularly due to the methods used to purify and
182 mechanically separate the cells, including filtrations and washings and, for some organs,
183 enzymatic cleavage with two different enzymes (collagenase and dispase) were performed for
184 cell purification. Theoretically, after all these treatments related to organ dissociation, only a
185 few bacteria would remain adhered, suggesting that the large majority were intracellular.
186 However, in order to confirm this, cell sorting based on the labeling of the cells and confocal
187 analyzes were carried out for each cell type of each organ. For flow cytometry, regions
188 corresponding to infected cells were identified with the PE-cy5 canal and were set according to
189 uninfected control samples. The Alexa fluor 488 canal was used to identify the cell types
190 according to the isotype-control staining. One example for each cell type is given in S1 Fig, S2
191 Fig, S3 Fig, S4 Fig, S5 Fig and S6 Fig. Double-labeled cells were sorted using flow cytometry
192 and observed with confocal microscopy. A Z-stack was re-sliced horizontally and vertically to
193 obtain the projections of perpendicular views, confirming the intracellular presence of bacteria.
194 This allowed us to observe intracellular *Salmonella* expressing red tag, in green labeled cells
195 for all the cells considered. These results confirm the intracellular localization of the different
196 strains and thus validate our protocol designed to identify and quantify the cell types infected
197 by *Salmonella* in selected chick organs. Moreover, they show that *S. Typhimurium* can invade
198 all the cell types studied in this paper, i.e. monocytes-macrophages, B and T lymphocytes,

199 thrombocytes, epithelial and endothelial cells of chicks. Currently, only a few papers have
200 described the cells infected by *Salmonella in vivo* and most of these papers are in mouse models.
201 In these articles, *Salmonella* were found mainly in macrophages and neutrophils from the liver
202 and spleen of mice, but infected B and T lymphocytes were also identified (41-44).

203 A more detailed analysis of the confocal images allowed us to observe that in most
204 cases infected cells, whatever the cell type, only harbored one to five bacteria per cell (Fig 2),
205 but in a few, more bacteria were visualized. This result is consistent with results obtained in the
206 literature on *Salmonella* infected macrophages *in vivo*. Indeed, in many experiments in mice,
207 the majority of liver or spleen infected phagocytes contained relatively few bacteria (41-43,
208 45), but the presence of many bacteria per cells has also been reported (42, 45, 46). Our results
209 show that this heterogeneous number of bacteria per cell could be enlarged to non-phagocytic
210 cells in chicks. However, in mice it seems that the number of bacteria per cell had a moderate
211 impact on the infectious process as host cells that contain high numbers of bacteria have the
212 same probability of undergoing lysis as cells containing only a few bacteria (47). Both highly
213 and weakly infected cells contributed significantly to the *Salmonella* infection process and not
214 only the macrophages (43).

215

216 *Analysis of the infected cell types in the spleen*

217 In the chicken spleen, the distinction between the red and white pulp is less marked than
218 in mammals. The red pulp mainly contains erythrocytes, granulocytes, macrophages, scattered
219 T lymphocytes and plasma cells. However, the architecture of the avian white pulp differs
220 considerably. Three morphologically distinct areas constitute the spleen. The first consists of
221 peri-arteriolar lymphocyte sheaths, mainly containing T lymphocytes that surround arterioles,
222 which have visible muscular layers. The second involves peri-ellipsoid lymphocyte sheaths
223 (PELS) surrounding capillaries, lacking muscular tissue and lined by cuboidal endothelium and

224 reticulin fibers. The last consists of follicles with germinal centers, surrounded by a capsule of
225 connective tissue. PELS and follicles mainly contain B lymphocytes (48).

226 In the spleen, the six antibodies used in our study allowed us to detect about 86% of the
227 total cells. Epithelial cell labeling was not necessary, as these cells were not expected to be
228 present. B lymphocytes (average of 8%), T lymphocytes (average of 22%) and endothelial cells
229 (average of 30%) were identified the most, as expected (Fig 3A). Compared to the non-infected
230 chicks, the percentage of labeled cells was similar in the groups of chicks inoculated with the
231 wild-type bacteria, the single or triple mutant bacteria. The only statistical difference was
232 observed for the percentage of thrombocytes between the uninfected chicks and the chicks
233 infected with the wild-type strain ($p=0.049$. S1 Table). The small decrease in the number of
234 thrombocytes after infection with the wild-type strain, was similar to that observed with the two
235 mutants, but the number of independent experiments was probably not sufficient to obtain a
236 statistical difference between the uninfected group and the chicks inoculated with these
237 *Salmonella* mutants. Similarly, the lower percentage of macrophages observed after infection
238 with the 3 Δ mutant strain was not significant. Either the absence of cell recruitment is real in
239 chicks or it could be related more to the fact that the infected cells were identified only two
240 days after the intra-peritoneal inoculation. The infection rates observed for all the identified
241 cells (lymphocytes, macrophages, thrombocytes, and endothelial cells) were between 0.1 and
242 1%. Monocytes and macrophages were proportionally the most infected cells (about five times
243 more than the other cell types), but endothelial cells, and B and T lymphocyte cells were the
244 most infected cells in the spleen as their absolute number was higher than that of monocytes-
245 macrophages in this organ. No statistical differences were observed according to the *Salmonella*
246 strains tested (Fig 3B). The fact that monocytes-macrophages were identified as being
247 proportionally the most infected cells of the spleen was not surprising. In mice, it is commonly
248 assumed that the systemic spread of *Salmonella* is contingent upon dissemination and survival

249 within macrophages. Indeed, survival in macrophages is essential for virulence (49). However,
250 contrary to what was assumed, our work, clearly demonstrated that other cell types, such as
251 lymphocytes, thrombocytes and endothelial cells could also be infected by *Salmonella* in
252 chicken spleen. As monocytes and macrophages are phagocytic cells, the fact that there was no
253 difference in the percentage of monocyte-macrophage infected cells between the mutants and
254 the wild-type strain was to be expected. By contrast, B and T lymphocytes, thrombocytes and
255 endothelial cells are non-phagocytic cells and thus a difference in the percentage of cells
256 infected by the different strains could have been expected. However, Geddes *et al.* have also
257 described in mice the internalization of *Salmonella* in splenic B and T cells, independently of
258 the T3SS-1 (44). Our work suggests that this observation could be extended to other non-
259 phagocytic cells of other animal species.

260

261 *Analysis of the infected cell types in the liver*

262 The liver is divided into a right and a left lobe. Each lobe of the liver has approximately
263 100,000 lobules separated from each other by interlobular *septum*. These lobules are formed by
264 parenchymal cells (hepatocytes), which represent 80% of the total liver volume and non-
265 parenchymal cells localized in the sinusoidal wall. These sinusoidal walls are the vascular side
266 of the hepatocytes and they are composed of endothelial cells and macrophages. These
267 macrophages are star-shaped and confined to the liver. Called Kupffer cells, they phagocyte
268 pathogens, cell debris and damaged red and white blood cells (50).

269 In the liver, the six antibodies used allowed us to detect about 76% of the cells and we
270 detected as many epithelial cells (average of 31%) as endothelial cells (average of 33%) (Fig
271 4A). As expected, these were the main cell types identified. Few monocytes-macrophages were
272 identified. One hypothesis is that the KUL01 antibody poorly recognizes the Kupffer cells (51).
273 Another hypothesis is that their percentage compared to epithelial and endothelial cells is very

274 low in the liver. There were also very few, if any, T lymphocytes. In humans and mice,
275 lymphocytes are present in small quantities at the level of the sinusoids and the space of Disse
276 (perisinusoidal space) and histological investigation does not suggest that there are many
277 immunologically relevant cells present (52). Liver-resident lymphocytes serve as sentinels and
278 perform immunosurveillance in response to infection and non-infectious insults, and are
279 involved in the maintenance of liver homeostasis (53). Our low level of T lymphocytes in the
280 liver is most probably related to the fact that our observations were made two days after the
281 intraperitoneal inoculation and that our chicks were only six days old and therefore
282 immunologically immature. For all cell types, in the liver, the percentage of labeled cells was
283 quite similar, whatever the infected or uninfected status of the animals. Only a statistical
284 difference for the percentages of labeled epithelial cells between the uninfected chicks and those
285 infected with the *invA* mutant was observed ($p=0.039$, S1 Table). Like in the spleen, we were
286 able to observe similar levels of infected cells between chicks inoculated with the wild-type
287 strain or with the two mutant strains deleted of the known entry factors. Compared to the spleen,
288 the percentages of labeled infected cells were more heterogeneous (Fig 4B). In particular, the
289 percentages of infected monocytes-macrophages and B lymphocytes were around 3%, while
290 the percentages of infected epithelial and endothelial cells were 0.10% and 0.24%, respectively.
291 Nevertheless, as these latter cell types are more frequent in the liver than monocytes-
292 macrophages and B lymphocytes (Fig 4A), endothelial and epithelial cells represent a large
293 proportion of the infected cells in the liver. The monocytes-macrophages of the liver are
294 responsible among others, for the phagocytosis of pathogens and thus, it is not surprising that
295 they were found infected, with no differences whatever the strain inoculated. In contrast, the
296 thrombocytes were very weakly infected here.

297 All together, these results strengthen those observed in the spleen, showing that at least
298 four different cell types, i.e. monocytes-macrophages, B lymphocytes, endothelial and
299 epithelial cells, were infected by *Salmonella* in the liver of chicks.

300

301 *Analysis of the infected cell types in the aortic vessels*

302 The term “aortic vessels” in our paper corresponds in fact to the aortic arch and the
303 brachiocephalic trunk. In contrast to mammals, two brachiocephalic trunks arise from the arch
304 of the aorta and give rise to the common carotid and subclavian arteries in birds (54). This
305 “organ” was chosen as a source of endothelial cells.

306 For this organ, only 55% of the cells were identified through flow cytometric analysis.
307 This low percentage of identified cells was mainly related to the presence of smooth muscle
308 fibers in vessels for which no any antibodies exist for the chicken. The *adventitia*, which is the
309 outer layer of the arterial wall, is made up of connective tissue and elastic fibers. It contains
310 capillary vessels vascularizing the arterial wall as well as nerve fibers of the sympathetic and
311 parasympathetic autonomic system. According to the size of the arteries, the media, which is
312 the middle layer of the arterial wall, is made up of collagen, elastin or smooth muscle fibers
313 allowing vasoconstriction. The *intima*, the inner layer of the arterial wall separated from the
314 media by the internal elastic limiter, is formed of the vascular endothelium (cell monolayer)
315 resting on a layer of connective tissue (55).

316 The percentages of labeled cells in aortic vessels according to the chick group illustrated
317 in Fig 5A were more dispersed than for the previous two organs, probably due to the treatment
318 of the aortic vessel with enzymes, which made extraction less easy. Monocytes-macrophages
319 and endothelial cells were the most representative type of cells labeled, but all cell types were
320 identified (Fig 5A). This is the first organ in which we could observe a difference between the
321 percentages of monocytes-macrophages according to the uninfected or infected status of the

322 animals. Contrary to the spleen and the liver, the percentage of labeled monocytes-macrophages
323 showed statistically significant differences between the uninfected chicks and those infected
324 with the wild-type strain, on one hand, ($p = 0.035$. S1 Table) and those infected with the 3 Δ
325 mutant, on the other hand ($p = 0.043$. S1 Table). Despite a high percentage of labeled
326 endothelial cells, few if any were infected. By contrast, all the other cell types were infected
327 and to a greater proportion than in the spleen and liver (Fig 5B). Indeed, compared to the spleen
328 and liver, the median percentage of each infected cell type in the aortic vessels, except
329 endothelial cells, varied from 1 to 10% versus 0.1 – 1% in the spleen or 0 to 3% in the liver.
330 Surprisingly, in some chicks more than 10% of lymphocytes, thrombocytes and epithelial cells
331 were infected.

332 These results clearly show that, like in the spleen and liver, numerous cell types are
333 infected in vessels.

334

335 *Analysis of the infected cell types in the gall bladder*

336 The avian gall bladder is attached to the right liver lobe. Histologically, the avian gall
337 bladder is composed of three *tunicae*. The first, the *tunica mucosa* is mainly lined with non-
338 ciliated simple columnar epithelium and consists of a layer of connective tissue with elastic and
339 muscle fibers. The second, the *tunica muscularis* consists of smooth muscle fibers and abundant
340 intervening connective tissue. The third, the *tunica serosa* consists of coarse collagen fiber and
341 elastic fibers. All epithelial cells are basally located and contain an oval nucleus. Bile is
342 synthesized in the hepatocytes and secreted into bile canaliculi located on the lateral surfaces
343 of adjoining liver cells (56). Relatively little is known about biliary secretion in birds due to the
344 complex anatomy in which bile enters the intestine via both hepato-enteric and cystico-enteric
345 ducts. In ruminants, pigs and poultry, there is relatively continuous secretion of bile into the
346 intestine (50).

347 About 75% of cells were identified with the available antibodies. Numerous
348 “unidentified cells” would most probably correspond to fibroblasts. Endothelial cell labeling
349 was not performed, as they were not expected to be found in the gall bladder. By contrast, all
350 other cell types were identified. The epithelial cells represented about 60% of the identified
351 cells and the percentages of thrombocytes and monocytes-macrophages were between 1 and
352 10% (Fig 6A). B and T lymphocytes were less present. As for the aortic vessels, the variability
353 between animals was considerable, certainly due to the breakdown of organs with different
354 enzymes, which made extraction less reproducible. As in the other organs (except for the
355 percentages of monocytes-macrophages in the aortic vessels), there were no differences in the
356 percentages of the labeled cells between uninfected and infected chicks. By comparing the
357 inoculated chicks, only one statistically significant difference was observed for the percentage
358 of T lymphocytes between the chicks inoculated with the single or the triple mutant ($p = 0.041$.
359 S1 Table). Immune cells were highly infected. For example, about 10% of the B and T
360 lymphocytes were infected by the different strains. Moreover, B and T lymphocytes in the gall
361 bladder were found to be more infected than in the other organs. The other identified cells were
362 infected between 1 and 10 % (Fig 6B). In all cases, except one, no statistical differences were
363 observed between the chicks inoculated with the wild-type or the mutant strains. The only
364 significant statistical difference was observed for the infected monocytes-macrophages between
365 the chicks infected with the wild-type strain and those infected with the *invA* mutant strain ($p =$
366 0.020 – S1 Table). This could be due to the fact that only two $\Delta invA$ -inoculated animals had
367 infected monocytes-macrophages, while the percentages of monocytes-macrophages were
368 similar for the five animals tested. Another interesting point is that the analyses of the infected
369 areas (labeled + unlabeled) highlighted the high cell invasion rates of the gall bladder (Tab 1).
370 Cumulating all experiments, after two days of infection, the median percentages of all infected

371 cells (labeled and unlabeled) in the gall bladder were 2.23%, 1% and 3.65% depending on the
372 strain inoculated, whereas in the spleen, for example, they were only 0.35%, 0.19% and 0.31%.

373 As this organ had never been described as a site of *Salmonella* colonization in chicks
374 and as it is described as an organ that is important for *Salmonella* persistence in mice and
375 humans (57, 58), we decided to observe the infected tissues using immunohistochemistry.
376 Microscopic analysis shows that bacteria were located in the epithelium just above the *mucosa*
377 of the gall bladder but also in the *lamina propria*, whatever the strain inoculated. Interestingly,
378 when high numbers of *Salmonella* were detected, the epithelium was damaged while the
379 structure of the gall bladder was well conserved when the tissue was only infected by a few
380 bacteria (Fig 7).

381 The gall bladder is thus colonized by *Salmonella* after chicks are inoculated via an
382 intraperitoneal route. These results show that oral inoculation of *Salmonella* is not necessary
383 for gall bladder infection. The bacteria reached the gall bladder through the vasculature or the
384 ducts that emanate from the liver. Menendez *et al.* obtained similar results in a mouse infection
385 model (59). Indeed, they demonstrated that gallbladder colonization was not the result of
386 *Salmonella* ascending directly from the gastrointestinal tract and their histological analyzes
387 supported the idea that bacteria were discharged from the liver into the gall bladder *via* the bile.
388 Concerning the infected cells in the chick gall bladder, monocytes-macrophages, B and T
389 lymphocytes, thrombocytes and epithelial cells of this organ were all infected at a relatively
390 high level compared to the other organs and epithelial cells were the most infected cell type.
391 Menendez *et. al* also observed in their mouse model that *Salmonella* localized preferentially
392 within epithelial cells of the gallbladder. However, bacteria were rarely seen within the *lamina*
393 *propria* (59). Our observations of some *S. Typhimurium* in the *mucosa* and *submucosa* and the
394 identification of infected monocytes-macrophages, B and T lymphocytes, and thrombocytes
395 demonstrate that epithelial cells are not the only cells infected in the gall bladder of chicks.

396 Whether this result is restricted to chicks or not remains to be determined. Our results on our
397 mutant strains are also different from that of Menendez *et al.* (59). Indeed, our mutants were
398 shown to infect similar cells to the wild-type, while Menendez *et al.* did not observe their *invA*
399 mutant in the epithelial cells of the murine gall bladder, in contrast to their wild-type strain,
400 suggesting that T3SS-1 could be required for *Salmonella* colonization of the gall bladder in
401 mice but not in chicks.

402 The gall bladder is known to be an organ in which *S. Typhi* persist during chronic
403 infections in humans, after forming a biofilm on gallstones (31, 58, 60). Models of chronic
404 infection in mice have also been studied (57, 59, 61). In guinea pigs, although asymptomatic,
405 *Salmonella* could be recovered in the gall bladder for up to 5 months post-infection (62).
406 However, it is not known whether this organ could be relevant for the persistence of *Salmonella*
407 in chicken.

408 Table 1. Percentages of infected cells (labeled and unlabeled) according to the organ

	Spleen	Liver	Aortic vessels	Gall bladder
	Median (Q1; Q3)	Median (Q1; Q3)	Median (Q1; Q3)	Median (Q1; Q3)
WT	0.35 (0.19; 0.53)	0.07 (0.06; 0.10)	0.64 (0.42; 2.49)	2.23 (1.54; 2.82)
$\Delta invA$	0.19 (0.14; 0.55)	0.06 (0.04; 0.16)	0.21 (0.12; 1.46)	1.00 (0.52; 2.71)
3 Δ	0.31 (0.26; 0.38)	0.06 (0.04; 0.16)	2.18 (1.18; 2.54)	3.65 (2.39; 4.62)

409

410

411 *Salmonella Typhimurium* is able to persist in the gall bladder independently of the T3SS1, Rck
412 and PagN.

413 As the previous results demonstrated that bacterial concentrations in the gall bladder
414 were significant (Fig 1) and that *Salmonella* was able to infect several cell types in this organ,
415 we verified whether this organ could be infected over the long term. To determine persistence

416 in this organ, we infected chicks and monitored their colonization rate in the spleen and gall
417 bladder for 36 days with slaughtering every 8 days. Bacteria were detected throughout the
418 kinetics. No statistical differences of colonization could be observed in the spleen (Fig 8A) or
419 in the gall bladder (Fig 8B), whatever the strain inoculated and the week of analysis. This work
420 demonstrates for the first time, that *Salmonella* Typhimurium could invade the gall bladder of
421 chicks at levels and durations similar to those observed in the spleen and thus, can be considered
422 as a site of colonization in addition to the spleen and the liver in chicks. In mice, during chronic
423 infection, mimicking human *S. Typhi* infection, the spleen and the gall bladder are considered
424 as organs of persistence and gall bladder colonization presumably leads to re-infection of the
425 intestine through bile secretion (46, 57, 63). Our results also demonstrated that, for the gall
426 bladder to be infected, an oral route of infection is not necessary, as demonstrated by Menendez
427 *et al.* in a mouse model (59). The role of this organ colonization needs to be analyzed further
428 especially in relation to *Salmonella* intestinal colonization and persistence.

429

430 **Concluding remarks**

431 This work demonstrates for the first time, that *S. Typhimurium* can invade *in vivo* a
432 large array of phagocytic and non-phagocytic cells of different organs and vessels in chicks.
433 These cells are immune cells but also epithelial and endothelial cells as previously demonstrated
434 *in vitro* with cell lines (30). Moreover, numerous unidentified cells were infected. This is due
435 to the lack of antibodies in chicken to identify among others, dendritic cells, fibroblasts, and
436 heterophils, which are also important cells for the spread of the bacterium (46, 64, 65).
437 Development of new antibodies is required for further studies in chicks. Nevertheless, our
438 results show a great difference between mice and chicks. In mice, phagocytic cells and
439 especially macrophages are the main cells in which *Salmonella* replicate in the liver and spleen
440 (41-43, 46). In chicks, the cell tropism in these organs, as well as in the gall bladder and vessels,

441 is more diverse as *Salmonella* were found intracellularly in monocytes-macrophages but also
442 in lymphocytes, endothelial cells and epithelial cells. Whether macrophages are the privileged
443 localization of *Salmonella* or not in organs other than the liver and spleen in mice remains to
444 be determined.

445 Even if *Salmonella* are able to invade numerous cells, specificity occurs depending on
446 the organ. Indeed, for example, during a *Salmonella* infection, epithelial cells appeared more
447 sensitive in the gall bladder than in the liver. In the same way, endothelial cells appeared more
448 sensitive in the spleen than in the aortic vessels.

449 Surprisingly, the two mutant strains used in this study, i.e. a T3SS-1 mutant strain and
450 a mutant strain defective for the three currently known invasion factors, were able to invade the
451 same host cells as the wild-type strain. The fact that the triple mutant strain enters numerous
452 host cells, *in vivo*, confirms our previous results suggesting the existence of unknown invasion
453 factors. Indeed, we previously demonstrated that, despite the invalidation of the T3SS-1, Rck
454 and PagN, *S. Typhimurium* remained able to invade, *in vitro*, some non-phagocytic cell lines
455 of several animal and tissue origins at a similarly high level as the wild-type (30). However, we
456 cannot conclude that the T3SS-1, PagN and Rck are not required for the invasion of chicken
457 cells as a redundant role of the different invasion factors may occur. These two hypotheses are
458 reinforced by our results of chicken infection demonstrating that chicks can be colonized at a
459 higher level by the two mutant strains than by their wild-type parent after intraperitoneal
460 inoculation. The absence of T3SS-1 requirement for chicken colonization has already been
461 observed (18-20) and this fact can now be broadened to the PagN and Rck invasins. However,
462 in order to demonstrate the redundant role or not of these entry factors, further studies are
463 necessary in chicks and other animals. Altogether, these results are important in the
464 understanding of the mechanisms of *Salmonella* pathogenesis, as it has been described that
465 depending on the entry mechanism, both bacterial behavior and host response are different (28)

466 and thus opening up new avenues of research. On the one hand, it raises the question as to
467 whether the bacterial factors required for chicken cell invasion of systemic sites are still
468 unknown and, if so, whether certain cell types are infected *in vivo* by a particular entry
469 mechanism. On the other hand, could the known invasion factors in chicks be redundant? In
470 addition, does this mean that because cells can be infected through multiple pathways in an
471 organ, their response is multiple? Further studies involving Tnseq-mutant library screenings
472 and single cell approaches would help to address these questions.

473

474 **Materials and methods**

475 **pFPV-TurboFP650 plasmid construction**

476 Gene encoding TurboFP650 was amplified from the plasmid pTurboFP650-N
477 (Evrogen, Euromedex, France) with primers TurboFP650-XbaI
478 5'TGCTCTTAGATTTAAGAAGGAGATATAGATATGGGAGAGGATAGCGAGCTG3'
479 and TurboFP650-SphI 5'CATGCATGCTTAGCTGTGCCCCAGTTTGCTAGG3'. Then, the
480 PCR product and the pFPV25.1 plasmid (66) were restricted by XbaI and SphI restriction
481 enzymes, ligated and transformed into *E. coli* MC1061 (67). pFPV-TurboFP650 recombinant
482 plasmids were selected on Trypticase Soya Agar (TSA - BioMérieux) containing 100 µg/mL
483 of carbenicillin (Sigma-Aldrich) and clones which showed a purple color were selected for
484 restriction analysis. Clones with good restriction profiles were then sequenced to confirm the
485 absence of mutations in the TurboFP650 coding sequence.

486

487 **Strains used and inocula preparation**

488 The pFPV-TurboFP650 plasmid was introduced in *S. Typhimurium* 14028 wild-type
489 (WT), the $\Delta invA::kan$ mutant ($\Delta invA$; T3SS-1 defective) or the $\Delta invA::kan \Delta pagN::cm \Delta rck$
490 mutant (3 Δ) (30).

491 To prepare the inocula, the strains were cultured in Trypticase Soya Broth (TSB -
492 BioMérieux) supplemented with carbenicillin 100 µg/mL for 24h at 37°C with shaking. The
493 cultures were centrifuged at 4500g for 20 min at 20°C and the pellets were suspended in
494 phosphate buffered saline (PBS) containing 50% glycerol. The bacterial suspensions were then
495 aliquoted, frozen and stored at -80°C. The frozen aliquots from the same initial inoculum were
496 used throughout the experiments.

497

498 **Ethics statement**

499 The experiments with chickens were carried out in strict accordance with French
500 legislation. All animal care and use adhered to French animal welfare laws. The protocols for
501 this study were approved by the French Ministry of Education, Higher Education and
502 Research (Ministère de l'Education Nationale, de l'Enseignement Supérieur et de la Recherche)
503 under the protocol number APAFIS #19834-2019031911108197 v3. The principles of
504 reduction, replacement and refinement were implemented in all the experiments. Chicks were
505 sacrificed by decapitation and bleeding.

506

507 **Experimental infection**

508 Five-day-old PA12 White Leghorn chicks, provided by the Experimental Platform for
509 Infectious Disease (UE 1277 - INRAE) were intraperitoneally inoculated with 0.2 mL of
510 bacterial suspension. On the day of inoculation, a frozen aliquot of the inoculum was thawed.
511 Bacteria concentrations were standardized turbidimetrically and diluted to a concentration of
512 6.10^7 CFU/0.2 mL in PBS. Chicks were maintained in medium isolator systems (0.83 m²) with
513 controlled environmental conditions (feed, water, temperature, air humidity and lighting
514 scheme) for two days before sacrifice by decapitation and bleeding. To follow the persistence
515 in the gall bladder, the inoculation dose was 3.10^7 CFU/chick, in order to reduce the mortality

516 of chicks observed with the higher dose. The kinetics of organ colonization was followed each
517 week over a period of 36 days.

518

519 **Enumeration of bacterial load in infected organs**

520 On the day of sacrifice, control animals of the same age (i.e. not inoculated) were
521 provided by the Experimental Platform for Infectious Disease. Spleens, livers, gall bladders and
522 the aortic vessels were collected aseptically from each animal for quantification of bacterial
523 load.

524 To determine the bacterial load, organs were homogenized in TSB and serial 10-fold
525 dilutions were plated on TSA or *Salmonella–Shigella* medium supplemented with carbenicillin
526 100 µg/mL. The colonies per plate were counted after incubation for 24 h at 37°C. Counts were
527 expressed as log (CFU) per g of organ.

528

529 **Preparation of cells for flow cytometry**

530 For the flow cytometric analyses, organ-specific samples were obtained by pooling the
531 spleens, livers, aortic vessels and gall bladders of the different chicks in Hanks' buffered saline
532 solution (HBSS) without Ca²⁺ and Mg²⁺ in the dark at 4°C in order to be able to analyze at least
533 200,000 cells for each organ. Independent infections were repeated at less three times. Gall
534 bladders and aortic vessels were cut into small pieces and samples put in collagenase A (0.3%
535 - Sigma) – dispase I (1 U/mL - Sigma) – HBSS for 30 min at 37°C. The whole purification
536 process was performed at 4°C. All organs were then homogenized in HBSS using syringe
537 plungers and filtered through 40-µm-mesh cell strainers (Falcon), before being transferred into
538 a 50-ml centrifuge. After centrifugation at 1000g for 15 min, cells were washed, resuspended
539 in HBSS at approximately 5.10⁶ – 1.10⁷ cells / mL and maintained in the dark at 4°C.

540

541 **Flow cytometric analyses**

542 Cells were characterized according to the antibodies available in poultry (S2 Table).
543 Mouse Anti-Chicken antibody, clone KUL01 specifically recognizes chicken monocytes,
544 macrophages and interdigitating cells (68). Anti- CT3 antibody targets the avian homolog of
545 the CD3-antigen, a common antigen used to identify T lymphocytes (69). Clone AV20 antibody
546 recognizes the antigen Bu-1, a chicken B-cell marker, commonly used to identify B
547 lymphocytes (70). Mouse anti-chicken CD41/61 clone 11C3 recognizes chicken integrin
548 CD41/61 that is expressed on chicken thrombocytes and cells of the thrombocyte lineage (71).
549 Mouse anti L-CAM antibody recognizes an 81 kDa N-terminal tryptic fragment of L-CAM, an
550 epithelial cell marker, from embryonic chicken liver plasma membranes (72) and last VE-
551 Cadherin is an intercellular junction marker of endothelial cells. This is a synthetic peptide
552 corresponding to Human VE-Cadherin amino acids from position 750 to the C-terminus
553 conjugated to keyhole limpet hemocyanin. Rabbit polyclonal antibody anti-VE-cadherin clone
554 reacts with mouse, chicken and human VE-Cadherin.

555 The anti-Bu-1 and the anti-CD3, that allow B and T lymphocytes to be identified, were
556 FITC conjugated. Antibodies that allow identification of monocytes-macrophages,
557 thrombocytes, epithelial and endothelial cells, required an Alexa Fluor™ 488 conjugated anti-
558 secondary anti-mouse or anti-rabbit antibodies. The endothelial cell samples were pre-treated
559 with 20% horse serum. The primary antibodies were incubated with cells for 90 min at 4°C in
560 the dark and then rinsed in HBSS. When necessary, secondary antibodies were added for 90
561 min at 4°C in the dark, and then rinsed. Appropriate isotype control antibodies (S2 Table) were
562 used to determine the levels of unspecific staining in all the experiments. Parallel samples were
563 stained with a Fixable Viability Dye Cell Staining eFluor 450 (eBioscience (65-0863)) to
564 determine the settings for a live cell gate based on light scatter properties. All samples were
565 then filtered through 60-µm nylon Blutex just before flow cytometric analyses were performed

566 using a BD LSR Fortessa™ X-20 (BD Biosciences, San Jose, CA, USA). BD FACSDiva™
567 software (v 8.0.2) was used to analyze the cytometric data. Infected and control samples were
568 manipulated under the same conditions.

569

570 **Identification and relative quantification of infected and non-infected cells by flow**
571 **cytometry**

572 For each sample, dot plots were analyzed. The intensity of green fluorescence (FITC or
573 Alexa Fluor™ 488) is on the vertical axis, plotted against the intensity of red fluorescence
574 (TurboFP650) on the horizontal axis. Labelled infected cells thus emitted both green and red
575 fluorescence. They were revealed as dots in the upper right-hand part of the graph. For each
576 experiment in each organ, a gate was determined removing inappropriate labeling - debris based
577 on morphological criteria. Regions were set according to uninfected control samples and
578 isotype-control staining. In order to have quantitative results, 200,000 events were analyzed for
579 each sample for all staining. Examples are provided for some cell-type/organ labeling (for
580 monocytes-macrophages (S1 Fig) and thrombocytes (S2 Fig) in the gall bladder, B lymphocytes
581 (S3 Fig) and T lymphocytes (S4 Fig) in the spleen, epithelial cells in the liver (S5 Fig) and
582 endothelial cells in the aortic vessels (S6 Fig)). Quantification of the percent of positively
583 labeled cells was then calculated by subtracting the number of cells in the control areas from
584 those in the positive labeled areas. The positive labeling areas of B and T lymphocytes cells
585 were established using a control mouse IgG1-FITC conjugate, whereas the positive labeling
586 areas of monocytes-macrophages, thrombocytes and epithelial cells were determined with a
587 control mouse IgG1-Alexa Fluor™ 488 conjugate. For the labeling of the endothelial cells, we
588 used rabbit IgG, followed by a secondary antibody, an anti-IgG-Alexa Fluor™ 488 conjugate.
589 The total percentages of infected cells, positive labeled or unlabeled were also determined. All

590 negative responses were scored at 0.001% to account for the threshold and allow for a
591 logarithmic representation of the results. The medians are represented by a red dash.

592

593 **Purification of the infected cells and confocal laser-scanning analysis**

594 Cells were sorted using a high-speed cell sorter, MoFlo Astrios^{EQ} (Beckman Coulter
595 Inc, Brea, CA, USA) equipped with four lasers: violet (405nm), blue (488nm), yellow-green
596 (561nm) and red (640nm) and placed under a class II biological safety cabinet. We used a nozzle
597 of 90 µm and selected a sheath pressure of 40 psi. Sorted cells were collected in 1.5 ml
598 Eppendorf tubes containing 350 µL of HBSS medium supplemented with 10% fetal calf serum
599 to limit cell stress.

600 After cell sorting, samples were deposited on glass coverslips and centrifuged with a
601 cytopspin at 200 rpm for 10 min. Cells were then fixed in formaldehyde 4% for 10 min. Nucleus
602 staining was performed with DAPI 1 µg/mL for 1 min and coverslips were mounted on slides
603 with fluorescent mounting medium (Dako). Cells were observed under a SP8 confocal laser-
604 scanning microscope equipped with an HCP PL APO 100x/1.44 Oil CORR CS immersion
605 objective (Leica). Z-stacks were re-sliced horizontally and vertically to obtain the projections
606 of perpendicular views from 3D images, providing a view of all bacteria in the cells, using Las
607 AF lite 2.6.3 build 8173 software (Leica).

608

609 **Immuno-histochemistry (IHC)**

610 Chick gall bladders were fixed in 4% buffered paraformaldehyde at 4°C for 24 h. They
611 were then processed by routine methods, paraffin embedded, cut in sections (thickness, 5 µm),
612 and stained for IHC with HRP detection. All samples were incubated at room temperature. The
613 primary antibody was an anti-*Salmonella* lipopolysaccharide marker: rabbit anti-*Salmonella*
614 O:4,5 (1/100 – D. Pasteur). The tissue sections were dewaxed in Histosol (Shandon,

615 Thermoscientific), rehydrated in a decreasing series of ethanol, rinsed and rehydrated in tap
616 water. Sections were treated with heat-induced epitope retrieval, 10mM Sodium Citrate buffer,
617 pH 6, 121°C, for 15 min. The tissues were then rinsed in tap water. The endogen peroxidase
618 was blocked in 1% hydrogen peroxide and methanol for 30 min. Preparations were rinsed in
619 PBS with 1% skimmed milk and 0.05% Tween 20 (PBSTM), blocked in 20% goat serum - 30%
620 fetal calf serum - PBS for 20 min. They were then incubated with a primary antibody for 60
621 min and rinsed in PBSTM, followed by N-Histofine rabbit, HRP (MMFRANCE) for 30 min.
622 At the end, samples were rinsed in PBSTM, incubated with chromogen (diaminobenzidine,
623 liquid DAB +, MMFrance) for 5 min, counterstained with hematoxylin of Harris (Merck,
624 Labellians), rinsed in tap water, dehydrated in successive ethanol baths (50°, 70°, 90° and
625 absolute, each for 2 min), cleared in histosol, and mounted on coverslips with Eukitt.

626 Tissues were examined and photographed with a light microscope Eclipse 80i, Nikon
627 with DXM 1200C digital camera (Nikon Instruments, Europe, Amsterdam, Netherlands) and
628 NIS-Elements D Microscope Imaging Software.

629

630 **Statistical analyses**

631 A Kruskal-Wallis Test was conducted to examine the differences in the levels of organ
632 colonization, followed by a Dunn's multiple comparisons test (GraphPad Prism version 6.07
633 for Windows, GraphPad Software, La Jolla California USA, www.graphpad.com). Significance
634 was * $p < 0.05$ and ** $p < 0.01$.

635 For the flow cytometric analyses, asymptotic two-sample Fisher-Pitman permutation
636 tests (One-Way-Test) were performed with R software, package Rcmdr version 2.5.3 (2019-
637 05-06). Significance was * $p < 0.05$ (<http://www.r-project.org>,
638 <http://socserv.socsci.mcmaster.ca/jfox/Misc/Rcmdr/>).

639

640 Acknowledgements

641 We would like to thank Jérôme Trotereau (SPVB, ISP unit, INRAE Val de Loire) who
642 participated in inoculating the chicks and the staff of the Experimental Platform for Infectious
643 Diseases of Institut National de Recherche pour l'Agriculture, l'Alimentation et
644 l'Environnement (PFIE, INRAE Val de Loire) for caring for the chicks and participating in the
645 experiments, and also P. Quéré (3IMo, ISP unit, INRAE Val de Loire) for her advice on the
646 labeling of the monocytes-macrophages. We are also grateful to T. Larcher (PANTher APEX,
647 INRAE – Oniris Nantes) for his advice and technical support.

648

649 References

- 650 1. WHO. World Health Organization. Foodborne Disease Burden Epidemiology Reference Group.
651 2015. WHO estimates of the global burden of foodborne diseases. World Health Organization. 2017.
- 652 2. ECDC Ea. The European Union summary report on trends and sources of zoonoses, zoonotic
653 agents and food-borne outbreaks in 2016. EFSA Journal. 2019;15(12):5077.
- 654 3. Ferrari RG, Rosario DKA, Cunha-Neto A, Mano SB, Figueiredo EES, Conte-Junior CA. Worldwide
655 epidemiology of *Salmonella serovars* in animal-based foods: a meta-analysis. Appl Environ Microbiol.
656 2019;85(14).
- 657 4. Rabinowitz PM, Conti LA. Human-clinical-medicine: clinical approaches to zoonoses, toxicants
658 and other shared health risks. 1st ed. Saunders Maryland Heights, MD, USA;2009.
- 659 5. Knight-Jones TJ, Mylrea GE, Kahn S. Animal production food safety: priority pathogens for
660 standard setting by the World Organisation for Animal Health. Rev Sci Tech. 2010;29(3):523-35.
- 661 6. Menanteau P, Kempf F, Trotereau J, Virlogeux-Payant I, Gitton E, Dalifard J, et al. Role of
662 systemic infection, cross contaminations and super-shedders in *Salmonella* carrier state in chicken.
663 Environ Microbiol. 2018;20(9):3246-60.
- 664 7. Ly KT, Casanova JE. Mechanisms of *Salmonella* entry into host cells. Cell Microbiol.
665 2007;9(9):2103-11.
- 666 8. Heffernan EJ, Wu L, Louie J, Okamoto S, Fierer J, Guiney DG. Specificity of the complement
667 resistance and cell association phenotypes encoded by the outer membrane protein genes *rck* from
668 *Salmonella* Typhimurium and *ail* from *Yersinia enterocolitica*. Infect Immun. 1994;62(11):5183-6.
- 669 9. Rosselin M, Virlogeux-Payant I, Roy C, Bottreau E, Sizaret PY, Mijouin L, et al. Rck of *Salmonella*
670 *enterica*, subspecies *enterica* serovar Enteritidis, mediates zipper-like internalization. Cell Res.
671 2010;20(6):647-64.
- 672 10. Lambert MA, Smith SG. The PagN protein of *Salmonella enterica* serovar Typhimurium is an
673 adhesin and invasin. BMC Microbiol. 2008;8:142.
- 674 11. Lambert MA, Smith SG. The PagN protein mediates invasion *via* interaction with proteoglycan.
675 FEMS Microbiol Lett. 2009;297(2):209-16.
- 676 12. Wiedemann A, Mijouin L, Ayoub MA, Barilleau E, Canepa S, Teixeira-Gomes AP, et al.
677 Identification of the epidermal growth factor receptor as the receptor for *Salmonella* Rck-dependent
678 invasion. FASEB journal : official publication of the Federation of American Societies for Experimental
679 Biology. 2016;30(12):4180-91.

- 680 13. Wallis TS, Galyov EE. Molecular basis of *Salmonella*-induced enteritis. *Mol Microbiol.*
681 2000;36(5):997-1005.
- 682 14. Jneid B, Moreau K, Plaisance M, Rouaix A, Dano J, Simon S. Role of T3SS-1 SipD Protein in
683 Protecting Mice against Non-typhoidal *Salmonella* Typhimurium. *PLoS Negl Trop Dis.*
684 2016;10(12):e0005207.
- 685 15. Galan JE, Curtiss R, 3rd. Cloning and molecular characterization of genes whose products allow
686 *Salmonella* Typhimurium to penetrate tissue culture cells. *PNAS.* 1989;86(16):6383-7.
- 687 16. Murray RA, Lee CA. Invasion genes are not required for *Salmonella enterica* serovar
688 Typhimurium to breach the intestinal epithelium: evidence that *Salmonella* pathogenicity island 1 has
689 alternative functions during infection. *Infect Immun.* 2000;68(9):5050-5.
- 690 17. Hapfelmeier S, Stecher B, Barthel M, Kremer M, Muller AJ, Heikenwalder M, et al. The
691 *Salmonella* pathogenicity island (SPI)-2 and SPI-1 type III secretion systems allow *Salmonella* serovar
692 Typhimurium to trigger colitis via MyD88-dependent and MyD88-independent mechanisms. *J*
693 *Immunol.* 2005;174(3):1675-85.
- 694 18. Sivula CP, Bogomolnaya LM, Andrews-Polymenis HL. A comparison of cecal colonization of
695 *Salmonella enterica* serotype Typhimurium in white leghorn chicks and *Salmonella*-resistant mice.
696 *BMC Microbiol.* 2008;8:182.
- 697 19. Rychlik I, Karasova D, Sebkova A, Volf J, Sisak F, Havlickova H, et al. Virulence potential of five
698 major pathogenicity islands (SPI-1 to SPI-5) of *Salmonella enterica* serovar Enteritidis for chickens. *BMC*
699 *Microbiol.* 2009;9:268.
- 700 20. Desin TS, Lam PK, Koch B, Mickael C, Berberov E, Wisner AL, et al. *Salmonella enterica* serovar
701 Enteritidis pathogenicity island 1 is not essential for but facilitates rapid systemic spread in chickens.
702 *Infect Immun.* 2009;77(7):2866-75.
- 703 21. Hu Q, Coburn B, Deng W, Li Y, Shi X, Lan Q, et al. *Salmonella enterica* serovar Senftenberg
704 human clinical isolates lacking SPI-1. *J Clin Microbiol.* 2008;46(4):1330-6.
- 705 22. Suez J, Porwollik S, Dagan A, Marzel A, Schorr YI, Desai PT, et al. Virulence gene profiling and
706 pathogenicity characterization of non-typhoidal *Salmonella* accounted for invasive disease in humans.
707 *PLoS One.* 2013;8(3):e58449.
- 708 23. Conner CP, Heithoff DM, Julio SM, Sinsheimer RL, Mahan MJ. Differential patterns of acquired
709 virulence genes distinguish *Salmonella* strains. *PNAS.* 1998;95(8):4641-5.
- 710 24. Dyszel JL, Smith JN, Lucas DE, Soares JA, Swearingen MC, Vross MA, et al. *Salmonella enterica*
711 serovar Typhimurium can detect acyl homoserine lactone production by *Yersinia enterocolitica* in mice.
712 *J Bacteriol.* 2010;192(1):29-37.
- 713 25. Ghosh S, Chakraborty K, Nagaraja T, Basak S, Koley H, Dutta S, et al. An adhesion protein of
714 *Salmonella enterica* serovar Typhi is required for pathogenesis and potential target for vaccine
715 development. *PNAS.* 2011;108(8):3348-53.
- 716 26. Tundup S, Kandasamy M, Perez JT, Mena N, Steel J, Nagy T, et al. Endothelial cell tropism is a
717 determinant of H5N1 pathogenesis in mammalian species. *PLoS Pathog.* 2017;13(3):e1006270.
- 718 27. Pereira SS, Trindade S, De Niz M, Figueiredo LM. Tissue tropism in parasitic diseases. *Open Biol.*
719 2019;9:190036.
- 720 28. Miao EA, Mao DP, Yudkovsky N, Bonneau R, Lorang CG, Warren SE, et al. Innate immune
721 detection of the type III secretion apparatus through the NLRC4 inflammasome. *PNAS.*
722 2010;107(7):3076-80.
- 723 29. Ryan KJ, Ray CGE. *Sherris Medical Microbiology: an introduction to infectious disease* (fourth
724 edition). New York: McGraw-Hill, USA; 2004.
- 725 30. Roche SM, Holbert S, Trotereau J, Schaeffer S, Georgeault S, Virlogeux-Payant I, et al.
726 *Salmonella* Typhimurium invalidated for the three currently known invasion factors keeps its ability to
727 invade several cell models. *Front Cell Infect Microbiol.* 2018;8:273.
- 728 31. Gonzalez-Escobedo G, Marshall JM, Gunn JS. Chronic and acute infection of the gall bladder by
729 *Salmonella* Typhi: understanding the carrier state. *Nat Rev Microbiol.* 2011;9(1):9-14.
- 730 32. Galan JE. *Salmonella* interactions with host cells: type III secretion at work. *Annu Rev Cell Dev*
731 *Biol.* 2001;17:53-86.

- 732 33. Coburn B, Sekirov I, Finlay BB. Type III secretion systems and disease. *Clin Microbiol Rev.*
733 2007;20(4):535-49.
- 734 34. McGhie EJ, Brawn LC, Hume PJ, Humphreys D, Koronakis V. *Salmonella* takes control: effector-
735 driven manipulation of the host. *Curr Opin Microbiol.* 2009;12(1):117-24.
- 736 35. Jones MA, Hulme SD, Barrow PA, Wigley P. The *Salmonella* pathogenicity island 1 and
737 *Salmonella* pathogenicity island 2 type III secretion systems play a major role in pathogenesis of
738 systemic disease and gastrointestinal tract colonization of *Salmonella enterica* serovar Typhimurium
739 in the chicken. *Avian Pathol.* 2007;36(3):199-203.
- 740 36. Pavlova B, Volf J, Ondrackova P, Matiasovic J, Stepanova H, Crhanova M, et al. SPI-1-encoded
741 type III secretion system of *Salmonella enterica* is required for the suppression of porcine alveolar
742 macrophage cytokine expression. *Vet Res.* 2011;42:16.
- 743 37. Sekirov I, Gill N, Jogova M, Tam N, Robertson M, de Llanos R, et al. *Salmonella* SPI-1-mediated
744 neutrophil recruitment during enteric colitis is associated with reduction and alteration in intestinal
745 microbiota. *Gut microbes.* 2010;1(1):30-41.
- 746 38. Zhao X, Tang X, Guo N, An Y, Chen X, Shi C, et al. Biochanin a enhances the defense against
747 *Salmonella enterica* infection through AMPK/ULK1/mTOR-mediated autophagy and extracellular traps
748 and reversing SPI-1-dependent macrophage (MPhi) M2 polarization. *Front Cell Infect Microbiol.*
749 2018;8:318.
- 750 39. Lou L, Zhang P, Piao R, Wang Y. *Salmonella* Pathogenicity Island 1 (SPI-1) and its complex
751 regulatory network. *Front Cell Infect Microbiol.* 2019;9:270.
- 752 40. Elsheimer-Matulova M, Varmuzova K, Kyrova K, Havlickova H, Sisak F, Rahman M, et al. *phoP*,
753 SPI1, SPI2 and *aroA* mutants of *Salmonella* Enteritidis induce a different immune response in chickens.
754 *Vet Res.* 2015;46:96.
- 755 41. Richter-Dahlfors A, Buchan AM, Finlay BB. Murine salmonellosis studied by confocal
756 microscopy: *Salmonella* Typhimurium resides intracellularly inside macrophages and exerts a cytotoxic
757 effect on phagocytes *in vivo*. *J Exp Med.* 1997;186(4):569-80.
- 758 42. Salcedo SP, Noursadeghi M, Cohen J, Holden DW. Intracellular replication of *Salmonella*
759 Typhimurium strains in specific subsets of splenic macrophages *in vivo*. *Cell Microbiol.* 2001;3(9):587-
760 97.
- 761 43. Sheppard M, Webb C, Heath F, Mallows V, Emilianus R, Maskell D, et al. Dynamics of bacterial
762 growth and distribution within the liver during *Salmonella* infection. *Cell Microbiol.* 2003;5(9):593-600.
- 763 44. Geddes K, Cruz F, Heffron F. Analysis of cells targeted by *Salmonella* type III secretion *in vivo*.
764 *PLoS Pathog.* 2007;3(12):e196.
- 765 45. Thone F, Schwanhauser B, Becker D, Ballmaier M, Bumann D. FACS-isolation of *Salmonella*-
766 infected cells with defined bacterial load from mouse spleen. *J Microbiol Methods.* 2007;71(3):220-4.
- 767 46. Watson KG, Holden DW. Dynamics of growth and dissemination of *Salmonella in vivo*. *Cell*
768 *Microbiol.* 2010;12(10):1389-97.
- 769 47. Mastroeni P, Grant A, Restif O, Maskell D. A dynamic view of the spread and intracellular
770 distribution of *Salmonella enterica*. *Nat Rev Microbiol.* 2009;7(1):73-80.
- 771 48. Jeurissen SH. Structure and function of the chicken spleen. *Res Immunol.* 1991;142(4):352-5.
- 772 49. Fields PI, Swanson RV, Haidaris CG, Heffron F. Mutants of *Salmonella* Typhimurium that cannot
773 survive within the macrophage are avirulent. *PNAS.* 1986;83(14):5189-93.
- 774 50. Zaefarian F, Abdollahi MR, Cowieson A, Ravindran V. Avian Liver: The Forgotten Organ. *Animals*
775 *(Basel).* 2019;9(2).
- 776 51. Hu T, Wu Z, Bush SJ, Freem L, Vervelde L, Summers KM, et al. Characterization of
777 subpopulations of chicken mononuclear phagocytes that express TIM4 and CSF1R. *J Immunol.*
778 2019;202(4):1186-99.
- 779 52. Mehal WZ, Azzaroli F, Crispe IN. Immunology of the healthy liver: old questions and new
780 insights. *Gastroenterology.* 2001;120(1):250-60.
- 781 53. Wang Y, Zhang C. The roles of liver-resident lymphocytes in liver diseases. *Front Immunol.*
782 2019;10:1582.




- 783 54. Erdogan S. The branching of the aortic arch in the Eurasian bittern (*Botaurus stellaris*, Linnaeus
784 1758). *Vet Med*. 2012;57(5):239-44.
- 785 55. Tucker WD, Arora Y, Mahajan K. Anatomy, Blood Vessels. In: StatPearls (Internet). Treasure
786 Island (FL): StatPearls Publishing2020, PMID: 2922226.
- 787 56. Iqbal J, Bhutto AL, Shah MG, Lochi GM, Hayat S, Ali N, et al. Gross anatomical and histological
788 studies on the liver of broiler. *J Appl Environ Biol Sci*. 2014;4(12):284-95.
- 789 57. Crawford RW, Rosales-Reyes R, Ramirez-Aguilar Mde L, Chapa-Azuela O, Alpuche-Aranda C,
790 Gunn JS. Gallstones play a significant role in *Salmonella spp.* gallbladder colonization and carriage.
791 *PNAS*. 2010;107(9):4353-8.
- 792 58. Di Domenico EG, Cavallo I, Pontone M, Toma L, Ensoli F. Biofilm producing *Salmonella* Typhi:
793 chronic colonization and development of gallbladder cancer. *Int J Mol Sci*. 2017;18(9).
- 794 59. Menendez A, Arena ET, Guttman JA, Thorson L, Vallance BA, Vogl W, et al. *Salmonella* infection
795 of gallbladder epithelial cells drives local inflammation and injury in a model of acute typhoid fever. *J*
796 *Infect Dis*. 2009;200(11):1703-13.
- 797 60. Gunn JS, Marshall JM, Baker S, Dongol S, Charles RC, Ryan ET. *Salmonella* chronic carriage:
798 epidemiology, diagnosis, and gallbladder persistence. *Trends Microbiol*. 2014;22(11):648-55.
- 799 61. Scanu T, Spaapen RM, Bakker JM, Pratap CB, Wu LE, Hofland I, et al. *Salmonella* manipulation
800 of host signaling pathways provokes cellular transformation associated with gallbladder carcinoma.
801 *Cell Host Microbe*. 2015;17(6):763-74.
- 802 62. Lavergne GM, James HF, Martineau C, Diena BB, Lior H. The guinea pig as a model for the
803 asymptomatic human typhoid carrier. *Lab Anim Sci*. 1977;27(5 Pt 2):806-16.
- 804 63. Gonzalez-Escobedo G, Gunn JS. Gallbladder epithelium as a niche for chronic *Salmonella*
805 carriage. *Infect Immun*. 2013;81(8):2920-30.
- 806 64. van Dijk A, Tersteeg-Zijderfeld MH, Tjeerdsma-van Bokhoven JL, Jansman AJ, Veldhuizen EJ,
807 Haagsman HP. Chicken heterophils are recruited to the site of *Salmonella* infection and release
808 antibacterial mature Cathelicidin-2 upon stimulation with LPS. *Mol Immunol*. 2009;46(7):1517-26.
- 809 65. Aiastrui A, Pucciarelli MG, Garcia-del Portillo F. *Salmonella enterica* serovar Typhimurium
810 invades fibroblasts by multiple routes differing from the entry into epithelial cells. *Infect Immun*.
811 2010;78(6):2700-13.
- 812 66. Valdivia RH, Falkow S. Bacterial genetics by flow cytometry: rapid isolation of *Salmonella*
813 Typhimurium acid-inducible promoters by differential fluorescence induction. *Mol Microbiol*.
814 1996;22(2):367-78.
- 815 67. Casadaban MJ, Cohen SN. Analysis of gene control signals by DNA fusion and cloning in
816 *Escherichia coli*. *J Mol Biol*. 1980;138(2):179-207.
- 817 68. Mast J, Goddeeris BM, Peeters K, Vandesande F, Berghman LR. Characterisation of chicken
818 monocytes, macrophages and interdigitating cells by the monoclonal antibody KUL01. *Vet Immunol*
819 *Immunopathol*. 1998;61(2-4):343-57.
- 820 69. Chen CL, Ager LL, Gartland GL, Cooper MD. Identification of a T3/T cell receptor complex in
821 chickens. *J Exp Med*. 1986;164(1):375-80.
- 822 70. Rothwell CJ, Vervelde, L., Davison, T.F. Identification of Bu-1 alloantigens using the monoclonal
823 antibody AV20. 1996. In: *Poultry Immunology* [Internet]. Carfax, Abindon, UK.
- 824 71. Lacoste-Eleau AS, Bleux C, Quere P, Coudert F, Corbel C, Kanellopoulos-Langevin C.
825 Biochemical and functional characterization of an avian homolog of the integrin GPIIb-IIIa present on
826 chicken thrombocytes. *Exp Cell Res*. 1994;213(1):198-209.
- 827 72. Gallin WJ, Edelman GM, Cunningham BA. Characterization of L-CAM, a major cell adhesion
828 molecule from embryonic liver cells. *PNAS*. 1983;80(4):1038-42.

829

830




831 **Figure legends**

832 **Fig 1. Level of different *S. Typhimurium* strains in organs of chicks after intra-**
833 **peritoneal inoculation**

834 Five-day-old chicks were intraperitoneally inoculated with around 6.10^7 CFU/chick
835 with *S. Typhimurium* 14028 turboFP650 wild-type strain (WT ), $\Delta invA::kan$ mutant
836 strain ($\Delta invA$; T3SS-1 defective ) or the $\Delta invA::kan \Delta pagN::cm \Delta rck$ mutant strain
837 (3 Δ ; T3SS-1, Rck, PagN defective ). Two days post-infection, spleens, livers, aortic
838 vessels and gall bladders were removed aseptically from each animal for quantification of
839 bacterial load. Results are expressed as number of bacteria per g of organ (log CFU per g of
840 organ). The medians are represented by a red dash. A Kruskal-Wallis Test was conducted,
841 followed by Dunn's multiple comparisons test (GraphPad Software). Significance was * $p <$
842 0.05 and ** $p <$ 0.01.

843




844 **Fig 2. Intracellular localization of *Salmonella* in cells purified from *in vivo* infected organs**

845 Five-day-old chicks were intraperitoneally inoculated with around 6.10^7 CFU/chick
846 with *S. Typhimurium* 14028 turboFP650 wild-type strain (WT ), $\Delta invA::kan$ mutant
847 strain ($\Delta invA$; T3SS-1 defective ) or the $\Delta invA::kan \Delta pagN::cm \Delta rck$ mutant strain
848 (3 Δ ; T3SS-1, Rck, PagN defective ). Two days post infection, animals were sacrificed
849 and the different organs removed. After, cells were isolated from organs, they were sorted using
850 a high-speed cell sorter, MoFlo Astrios EQ and deposited on glass coverslips after cytopsin at
851 200 rpm for 10 min. Cells were then fixed in formaldehyde. Nucleus staining was performed
852 with Dapi (blue). The bacteria are in red (turboFP650), whereas cells are identified in green
853 thanks to FITC or Alexa FluorTM 488 conjugated antibodies. Cells were observed under a SP8
854 confocal laser-scanning microscope equipped with a 100x oil immersion objective (Leica). Z-
855 stacks were re-sliced horizontally and vertically to obtain the projections of perpendicular views

856 from 3D images, allowing a view of all bacteria in the cells, using Las AF lite 2.6.3 build 8173
857 software (Leica). White dashes represent 20 μm . **A** represents endothelial cells from the aortic
858 vessels, infected with the 3 Δ strain. Picture size 32.54 μm x 38.45 μm . **B** represents monocytes-
859 macrophages from the liver, infected with the $\Delta invA$ strain. Picture size 116.25 μm x 116.25
860 μm . **C** represents B lymphocytes, infected with the wild-type strain. Picture size 58.13 μm x
861 58.13 μm . **D** represents T lymphocytes, infected with the wild-type strain. Picture size 39.88
862 μm x 39.88 μm . **E** represents epithelial cells in the gall bladder, infected with the 3 Δ strain.
863 Picture size 37.80 μm x 37.80 μm . **F** represents thrombocytes in the aortic vessels, infected
864 with the 3 Δ strain. Picture size 116.25 μm x 116.25 μm .




865

866 **Fig 3. Percentage of identified and *Salmonella* infected cells in spleen**

867 Five-day-old chicks were intraperitoneally inoculated with around 6.10^7 CFU/chick
868 with *S. Typhimurium* 14028 turboFP650 wild-type strain (WT ), $\Delta invA::kan$ mutant
869 strain ($\Delta invA$; T3SS-1 defective ) or the $\Delta invA::kan \Delta pagN::cm \Delta rck$ mutant strain
870 (3 Δ ; T3SS-1, Rck, PagN defective ). Two days post infection, animals were sacrificed
871 and the different organs removed. Cells from uninfected animals of the same age were used as
872 a control. After labeling with the corresponding antibodies, the percentages of macrophages-
873 monocytes, B and T lymphocytes, thrombocytes and epithelial and endothelial cells were
874 quantified by flow-cytometry. The percentage of labeled cells (A) and the percentage of labeled
875 infected cells (B) are represented. All negative responses were scored at 0.001%. The medians
876 are represented by a red dash. Asymptotic two-sample Fisher-Pitman permutation tests (One-
877 Way-Test) were performed (R software). Significance was * $p < 0.05$.




878

879 **Fig 4. Percentage of identified and *Salmonella* infected cells in liver**

880 Five-day-old chicks were intraperitoneally inoculated with around 6.10^7 CFU/chick
881 with *S. Typhimurium* 14028 turboFP650 wild-type strain (WT ), $\Delta invA::kan$ mutant
882 strain ($\Delta invA$; T3SS-1 defective ) or the $\Delta invA::kan \Delta pagN::cm \Delta rck$ mutant strain
883 (3 Δ ; T3SS-1, Rck, PagN defective ). Two days post infection, animals were sacrificed
884 and the different organs removed. Cells from uninfected animals of the same age were used as
885 a control. After labeling with the corresponding antibodies, the percentages of macrophages-
886 monocytes, B and T lymphocytes, thrombocytes and epithelial and endothelial cells were
887 quantified by flow-cytometry. The percentage of labeled cells (A) and the percentage of labeled
888 infected cells (B) are represented. All negative responses were scored at 0.001%. The medians
889 are represented by a red dash. Asymptotic two-sample Fisher-Pitman permutation tests (One-
890 Way-Test) were performed (R software). Significance was * $p < 0.05$.




891

892 **Fig 5. Percentage of identified and *Salmonella* infected cells in aortic vessels**

893 Five-day-old chicks were intraperitoneally inoculated with around 6.10^7 CFU/chick
894 with *S. Typhimurium* 14028 turboFP650 wild-type strain (WT ), $\Delta invA::kan$ mutant
895 strain ($\Delta invA$; T3SS-1 defective ) or the $\Delta invA::kan \Delta pagN::cm \Delta rck$ mutant strain
896 (3 Δ ; T3SS-1, Rck, PagN defective ). Two days post infection, animals were
897 sacrificed and the different organs removed. Cells from uninfected animals of the same age
898 were used as a control. After labeling with the corresponding antibodies, the percentages of
899 macrophages-monocytes, B and T lymphocytes, thrombocytes and epithelial and endothelial
900 cells were quantified by flow-cytometry. The percentage of labeled cells (A) and the percentage
901 of labeled infected cells (B) are represented. All negative responses were scored at 0.001%. The
902 medians are represented by a red dash. Asymptotic two-sample Fisher-Pitman permutation tests
903 (One-Way-Test) were performed (R software). Significance was * $p < 0.05$.

904

905 **Fig 6. Percentage of identified and *Salmonella* infected cells in gall bladder**

906 Five-day-old chicks were intraperitoneally inoculated with around 6.10^7 CFU/chick
907 with *S. Typhimurium* 14028 turboFP650 wild-type strain (WT ), $\Delta invA::kan$ mutant
908 strain ($\Delta invA$; T3SS-1 defective ) or the $\Delta invA::kan \Delta pagN::cm \Delta rck$ mutant strain
909 (3Δ ; T3SS-1, Rck, PagN defective ). Two days post infection, animals were
910 sacrificed and the different organs removed. Cells from uninfected animals of the same age
911 were used as a control. After labeling with the corresponding antibodies, the percentages of
912 macrophages-monocytes, B and T lymphocytes, thrombocytes and epithelial and endothelial
913 cells were quantified by flow-cytometry. The percentage of labeled cells (A) and the percentage
914 of labeled infected cells (B) are represented. All negative responses were scored at 0.001%. The
915 medians are represented by a red dash. Asymptotic two-sample Fisher-Pitman permutation tests
916 (One-Way-Test) were performed (R software). Significance was * $p < 0.05$.

917




918 **Fig 7. Immunohisto-chemistry of chick gall bladder infected with *S. Typhimurium* wild-**
919 **type stain or with a mutant deleted of the three known invasion factors**

920 Five-day-old chicks were intraperitoneally inoculated with around 6.10^7 CFU/chick
921 with *S. Typhimurium* 14028 turboFP650 wild-type strain (WT) or the $\Delta invA::kan \Delta pagN::cm$
922 Δrck mutant strain (3Δ). Two days post infection, animals were sacrificed. Gall bladders were
923 removed and fixed in 4% buffered paraformaldehyde at 4°C for 24 h. Tissues were processed
924 using routine methods, paraffin embedded, cut in sections (thickness, 5 μ m), and stained with
925 diaminobenzidine for IHC with HRP detection. The primary antibody was a rabbit anti-
926 *Salmonella* O:4,5 lipopolysaccharide marker. Tissues were examined and photographed with a
927 light microscope Eclipse 80i, Nikon with DXM 1200C digital camera (Nikon Instruments,
928 Europe, Amsterdam, Netherlands) and NIS-Elements D Microscope Imaging Software. Tissues
929 were counterstained in blue with Harris' hematoxylin of and *Salmonella* were stained in brown

930 with HRP detection. Representative pictures are presented. Bacteria are seen (\blacktriangleright) within the
931 epithelium (e) and the mucosa (ma). Sections of a gall bladder of (A) an uninfected chick, (B,
932 D and E) a chick infected by the wild-type strain, (C and F) a chick infected by the 3Δ mutant
933 are represented.

934

935 **Fig 8. Persistence of *S. Typhimurium* in the spleen and in the gall bladder after**
936 **intraperitoneal inoculation**

937 Five-day-old chicks were intraperitoneally inoculated with around 3.10^7 CFU/chick
938 with *S. Typhimurium* 14028 turboFP650 wild-type (WT ), $\Delta invA::kan$ mutant strain
939 ($\Delta invA$; T3SS-1 defective ) or the $\Delta invA::kan \Delta pagN::cm \Delta rck$ mutant strain (3Δ ;
940 T3SS-1, Rck, PagN defective ). Each week, seven animals were sacrificed and their
941 spleens and gall bladders removed. The kinetics of spleen (A) and gall bladder (B) colonization
942 were followed each week for a period of 36 days. Results are expressed as number of bacteria
943 (log CFU per g of organ). The medians are represented by a red dash. A Kruskal-Wallis test
944 was conducted, followed by a Dunn's multiple comparisons test (GraphPad Software).
945 Significance was * $p < 0.05$.

946

947 **S1 Fig. Identification of labeled and infected labeled monocytes-macrophages using flow-**
948 **cytometry**

949 The antibody allowing identification of monocytes-macrophages required a secondary
950 Alexa FluorTM 488 conjugated anti-mouse antibody. Flow cytometric analyses were performed
951 with a BD LSR FortessaTM X-20 (BD Biosciences, San Jose, CA, USA). BD FACSDivaTM
952 software (v 8.0.2) was used to analyze the cytometric data. For each sample, dot plots were
953 analyzed. Debris was removed on the basis of morphological criteria, regions were defined on
954 the basis of uninfected control samples and isotype-control staining. The intensity of green

955 fluorescence (Alexa Fluor™ 488) was on the vertical axis, plotted against the intensity of red
956 fluorescence (TurboFP650) on the horizontal axis. Labeled cells emitting a green fluorescence
957 were detected in the upper part of the graph. Infected labeled cells emitting both types of
958 fluorescence (green and red) were revealed by dots in the upper right-hand part of the graph.
959 Unlabeled infected cells could also be seen in the lower right-hand part of the graph. Results
960 were expressed as a percentage. Some examples are presented. Staining in the gall bladder is
961 shown for the monocytes-macrophages.

962

963 **S2 Fig. Identification of labeled and infected labeled thrombocytes using flow-cytometry**

964 The antibody allowing identification of thrombocytes required a secondary Alexa
965 Fluor™ 488 conjugated anti-mouse antibody. Flow cytometric analyses were performed with a
966 BD LSR Fortessa™ X-20 (BD Biosciences, San Jose, CA, USA). BD FACSDiva™ software
967 (v 8.0.2) was used to analyze the cytometric data. For each sample, dot plots were analyzed.
968 Debris was eliminated on the basis of morphological criteria, regions were set according to
969 uninfected control samples and isotype-control staining. The intensity of green fluorescence
970 (Alexa Fluor™ 488) is on the vertical axis, plotted against the intensity of red fluorescence
971 (TurboFP650) on the horizontal axis. Labeled cells emitting a green fluorescence were detected
972 in the upper part of the graph. Infected labeled cells emitting both types of fluorescence (green
973 and red) were revealed by dots in the upper right-hand part of the graph. Unlabeled infected
974 cells could also be seen in the lower right-hand part of the graph. Results were expressed as a
975 percentage. Some examples are presented. Staining in the gall bladder is shown for the
976 thrombocytes.

977

978 **S3 Fig. Identification of labeled and infected labeled monocytes-macrophages using flow-** 979 **cytometry**

980 The anti-Bu antibody, that allows B lymphocytes identification, was FITC conjugated.
981 Flow cytometric analyses were performed with a BD LSR Fortessa™ X-20 (BD Biosciences,
982 San Jose, CA, USA). BD FACSDiva™ software (v 8.0.2) was used to analyze the cytometric
983 data. For each sample, dot plots were analyzed. Debris was eliminated on the basis of
984 morphological criteria, regions were set according to uninfected control samples and isotype-
985 control staining. The intensity of green fluorescence (FITC) is on the vertical axis, plotted
986 against the intensity of red fluorescence (TurboFP650) on the horizontal axis. Labeled cells
987 emitting a green fluorescence were detected in the upper part of the graph. Infected labeled cells
988 emitting both types of fluorescence (green and red) were revealed by dots in the upper right-
989 hand part of the graph. Unlabeled infected cells could also be seen in the lower right-hand part
990 of the graph. Results are expressed as percentages. Some examples are presented. Staining in
991 the spleen is shown for the B lymphocytes.

992

993 **S4 Fig. Identification of labeled and infected labeled T lymphocytes using flow-cytometry**

994 The anti-CD3 antibody, that allows T lymphocytes identification, was conjugated with
995 FITC. Flow cytometric analyses were performed with a BD LSR Fortessa™ X-20 (BD
996 Biosciences, San Jose, CA, USA). BD FACSDiva™ software (v 8.0.2) was used to analyze the
997 cytometric data. For each sample, dot plots were analyzed. Debris was eliminated on the basis
998 of morphological criteria, regions were set according to uninfected control samples and isotype-
999 control staining. The intensity of green fluorescence (FITC) is on the vertical axis, plotted
1000 against the intensity of red fluorescence (TurboFP650) on the horizontal axis. Labeled cells
1001 emitting a green fluorescence were detected in the upper part of the graph. Infected labeled
1002 cells emitting both types of fluorescence (green and red) were revealed by dots in the upper
1003 right-hand part of the graph. Unlabeled infected cells could also be seen in the lower right-hand

1004 part of the graph. Results are expressed as percentages. Some examples are presented. Staining
1005 in the spleen is shown for the T lymphocytes.

1006

1007 **S5 Fig. Identification of labeled and infected labeled epithelial cells using flow-cytometry**

1008 The antibody allowing identification of epithelial cells required a secondary Alexa
1009 Fluor™ 488 conjugated anti-mouse antibody. Flow cytometric analyses were performed with a
1010 BD LSR Fortessa™ X-20 (BD Biosciences, San Jose, CA, USA). BD FACSDiva™ software
1011 (v 8.0.2) was used to analyze the cytometric data. For each sample, dot plots were analyzed.
1012 Debris was eliminated on the basis of morphological criteria, regions were set according to
1013 uninfected control samples and isotype-control staining. The intensity of green fluorescence
1014 (Alexa Fluor™ 488) is on the vertical axis, plotted against the intensity of red fluorescence
1015 (TurboFP650) on the horizontal axis. Labeled cells emitting a green fluorescence were detected
1016 in the upper part of the graph. Infected labeled cells emitting both types of fluorescence (green
1017 and red) were revealed by dots in the upper right-hand part of the graph. Unlabeled infected
1018 cells could also be seen in the lower right-hand part of the graph. Results are expressed as
1019 percentages. Some examples are presented. Staining in the liver is shown for epithelial cells.

1020

1021 **S6 Fig. Identification of labeled and infected labeled endothelial cells using flow-**
1022 **cytometry**

1023 The antibody allowing identification of endothelial cells required a secondary Alexa
1024 Fluor™ 488 conjugated anti-rabbit antibody. Flow cytometric analyses were performed with a
1025 BD LSR Fortessa™ X-20 (BD Biosciences, San Jose, CA, USA). BD FACSDiva™ software
1026 (v 8.0.2) was used to analyze the cytometric data. For each sample, dot plots were analyzed.
1027 Debris was eliminated on the basis of morphological criteria, regions were set according to
1028 uninfected control samples and isotype-control staining. The intensity of green fluorescence
1029 (Alexa Fluor™ 488) is on the vertical axis, plotted against the intensity of red fluorescence

1030 (TurboFP650) on the horizontal axis. Labeled cells emitting a green fluorescence were detected
1031 in the upper part of the graph. Infected labeled cells emitting both types of fluorescence (green
1032 and red) were revealed by dots in the upper right-hand part of the graph. Unlabeled infected
1033 cells could also be seen in the lower right-hand part of the graph. Results are expressed as
1034 percentages. Some examples are presented. Staining in the aortic vessels is shown for
1035 endothelial cells.

1036

Fig 1. Experimental infection of chicks by *Salmonella*

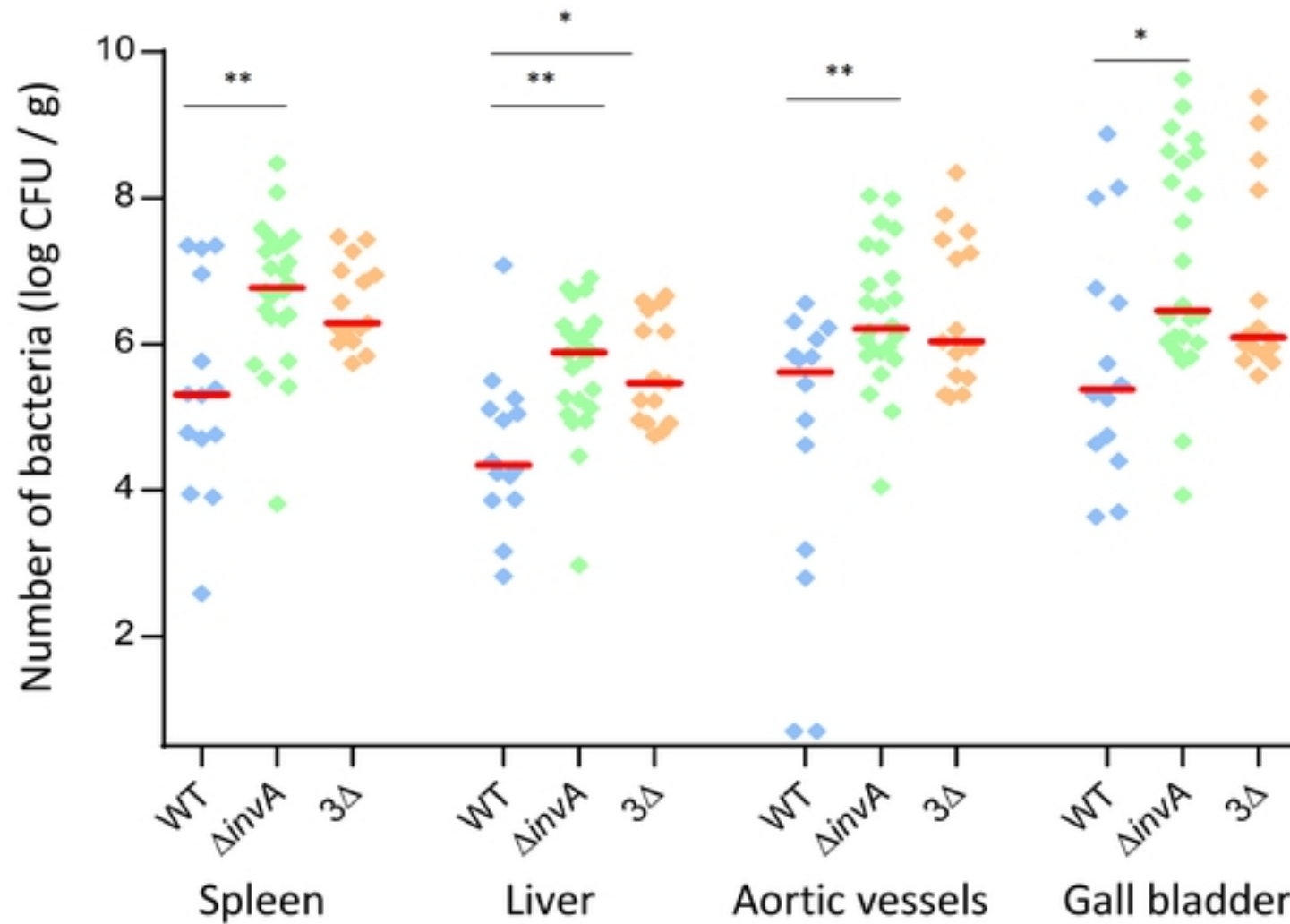
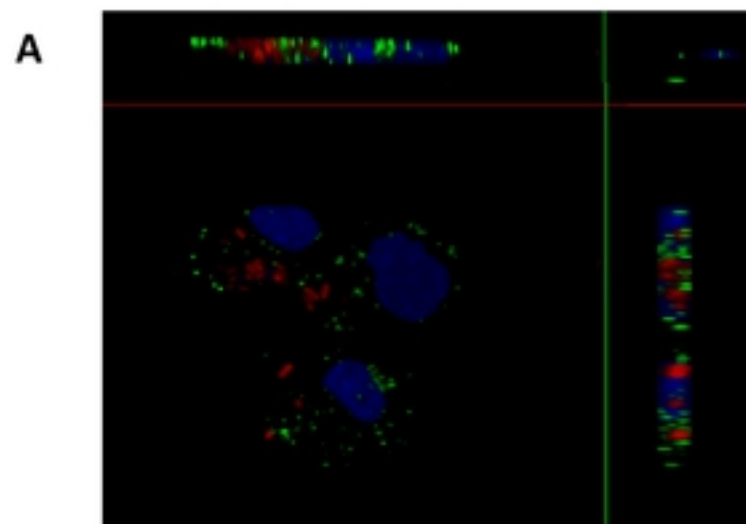
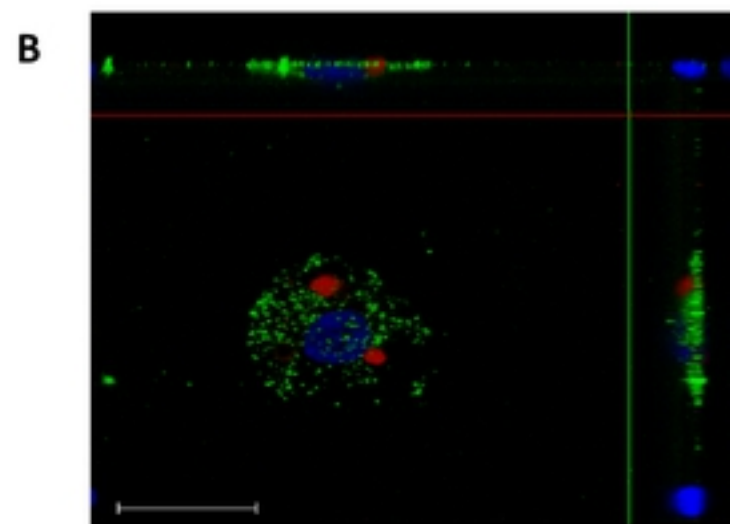


Figure 1

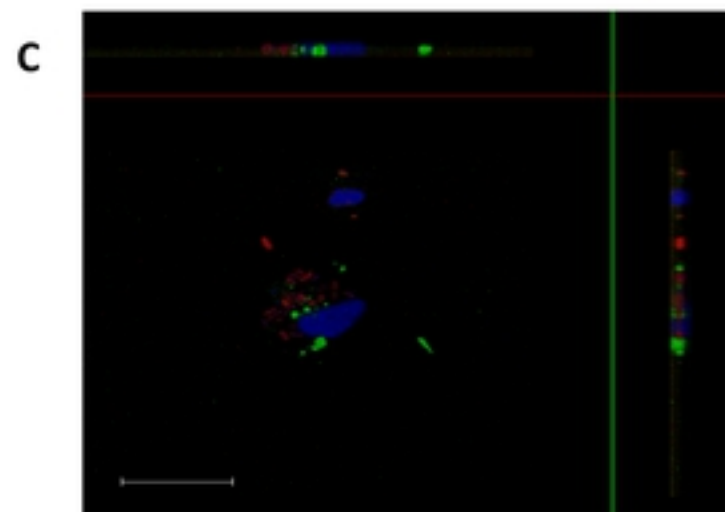
Fig. 2



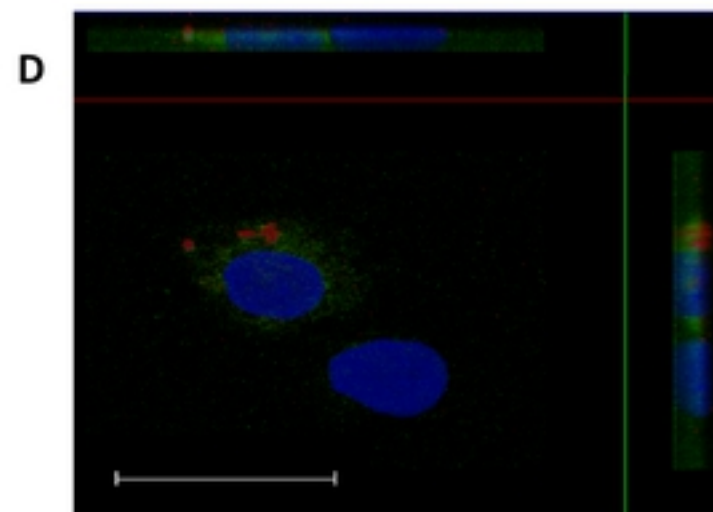
Endothelial cells



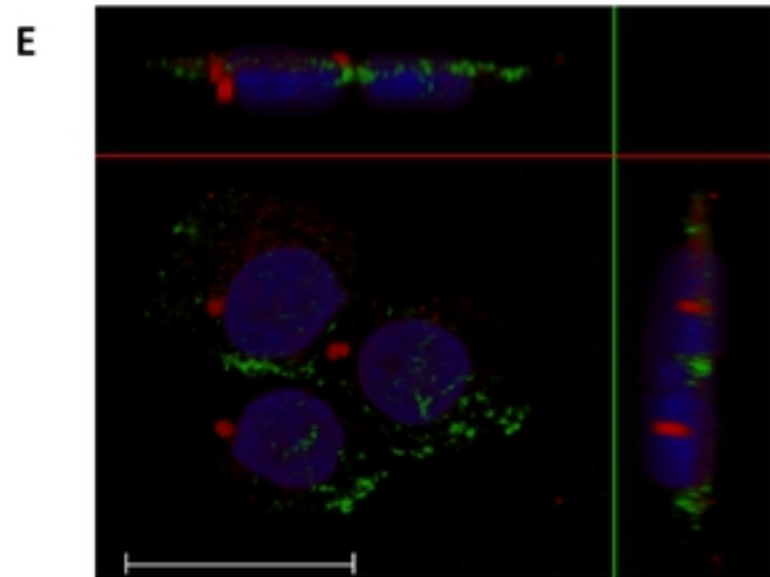
Monocytes-macrophages



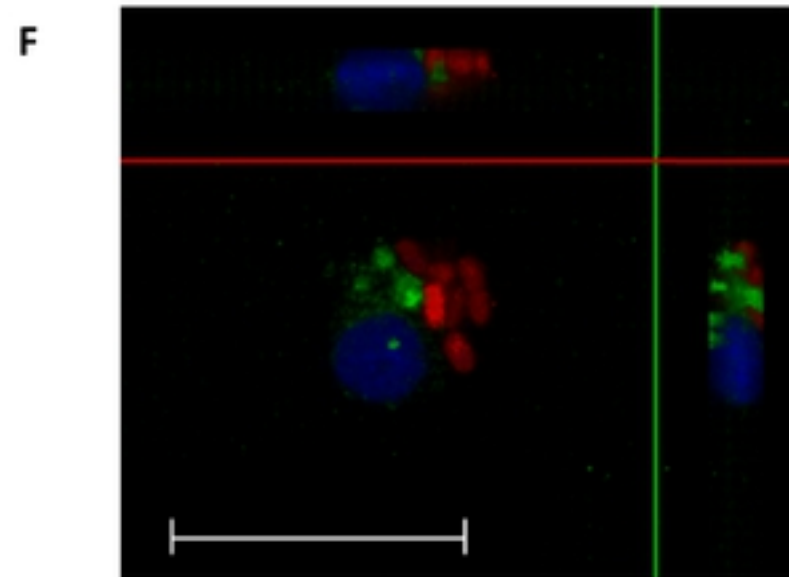
B lymphocytes



T lymphocytes



Epithelial cells



Thrombocytes

Fig 3. Cell types and *Salmonella* infected cells

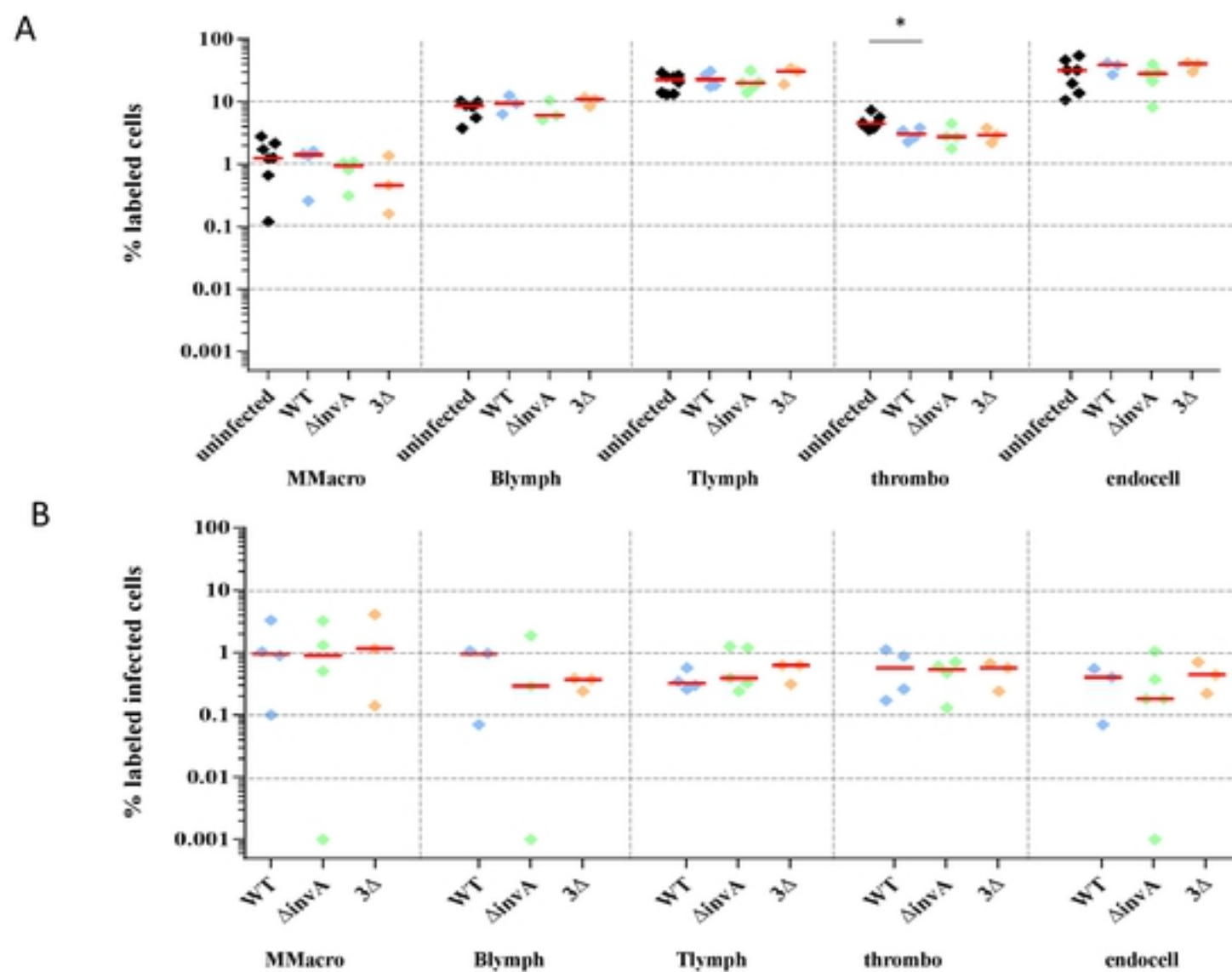


Figure 3

Fig 4. Cell types and *Salmonella* infected cells

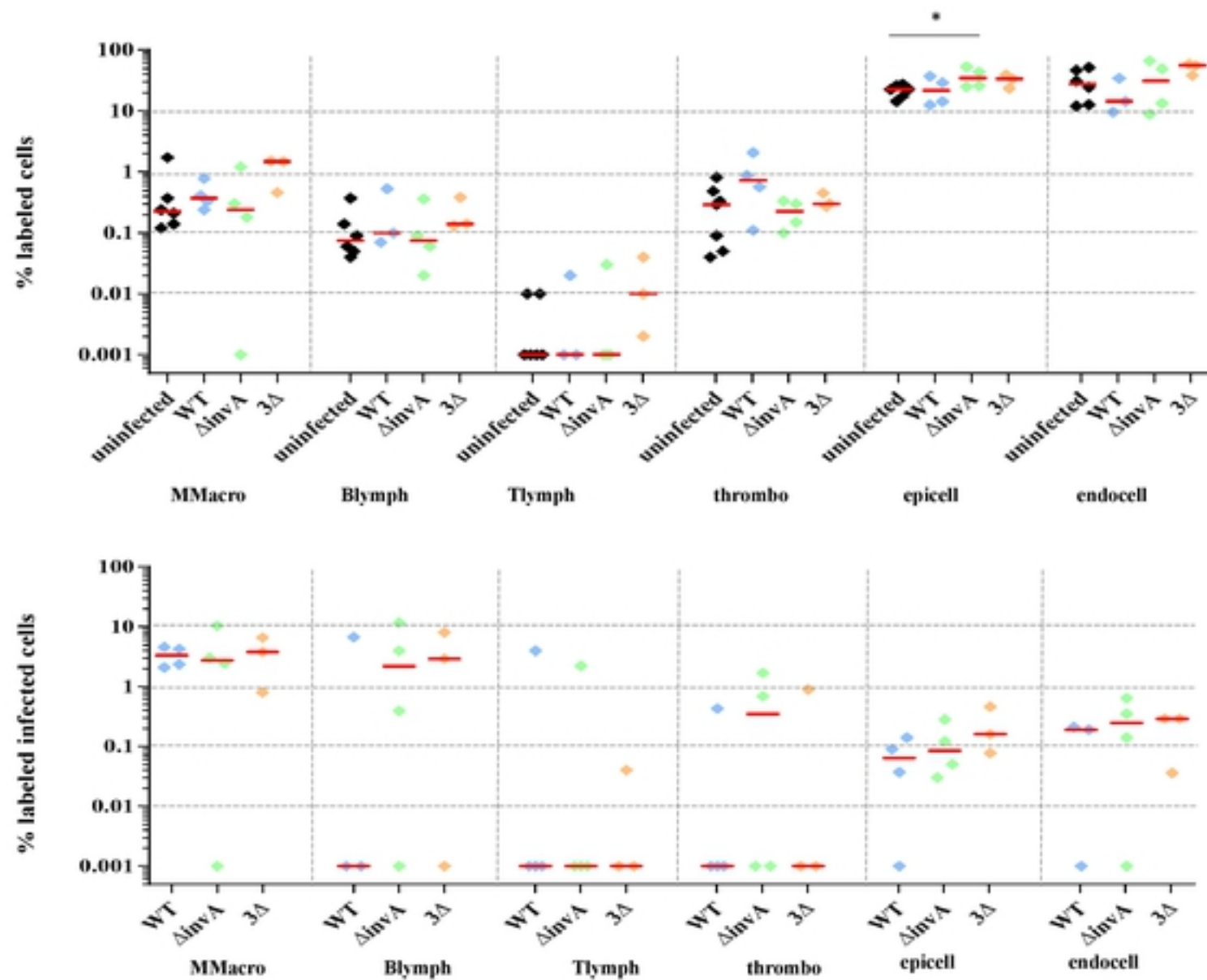


Figure 4

Fig 5. Cell types and *Salmonella* infected cells

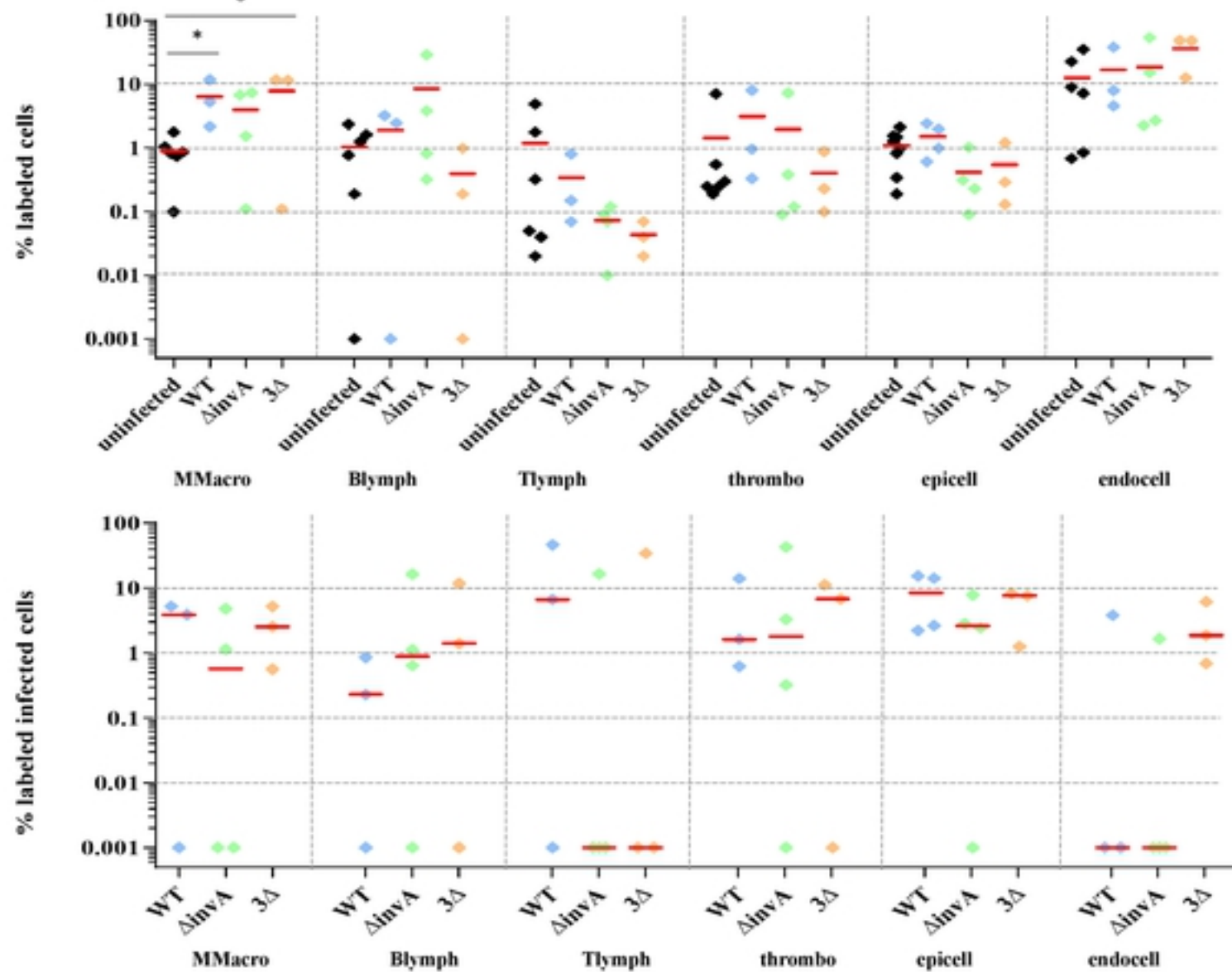


Figure 5

Fig 6. Cell types and *Salmonella* infected cells

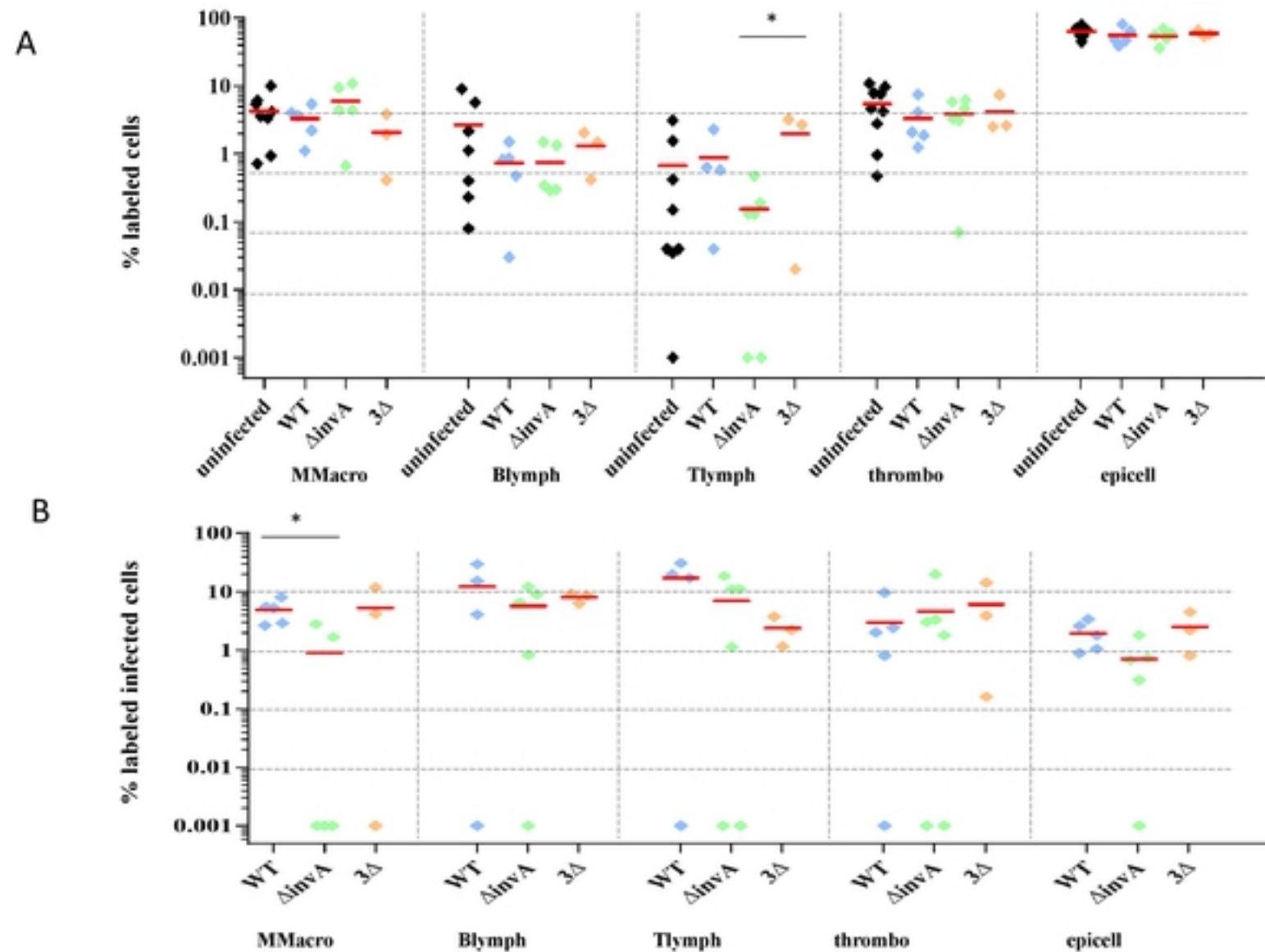


Figure 6

Fig 7. Immunohisto-chemistry of the chicks gall bladder

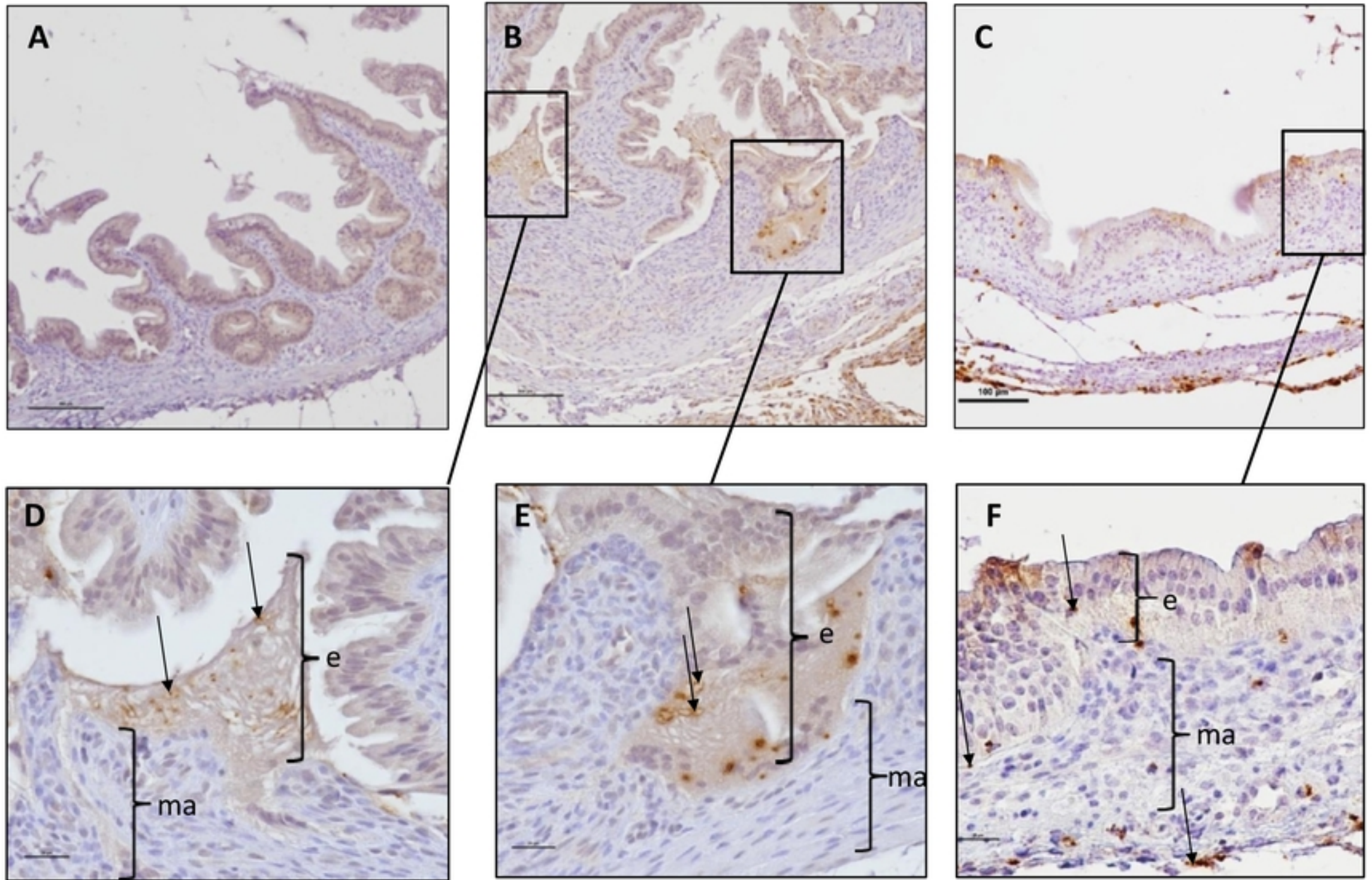
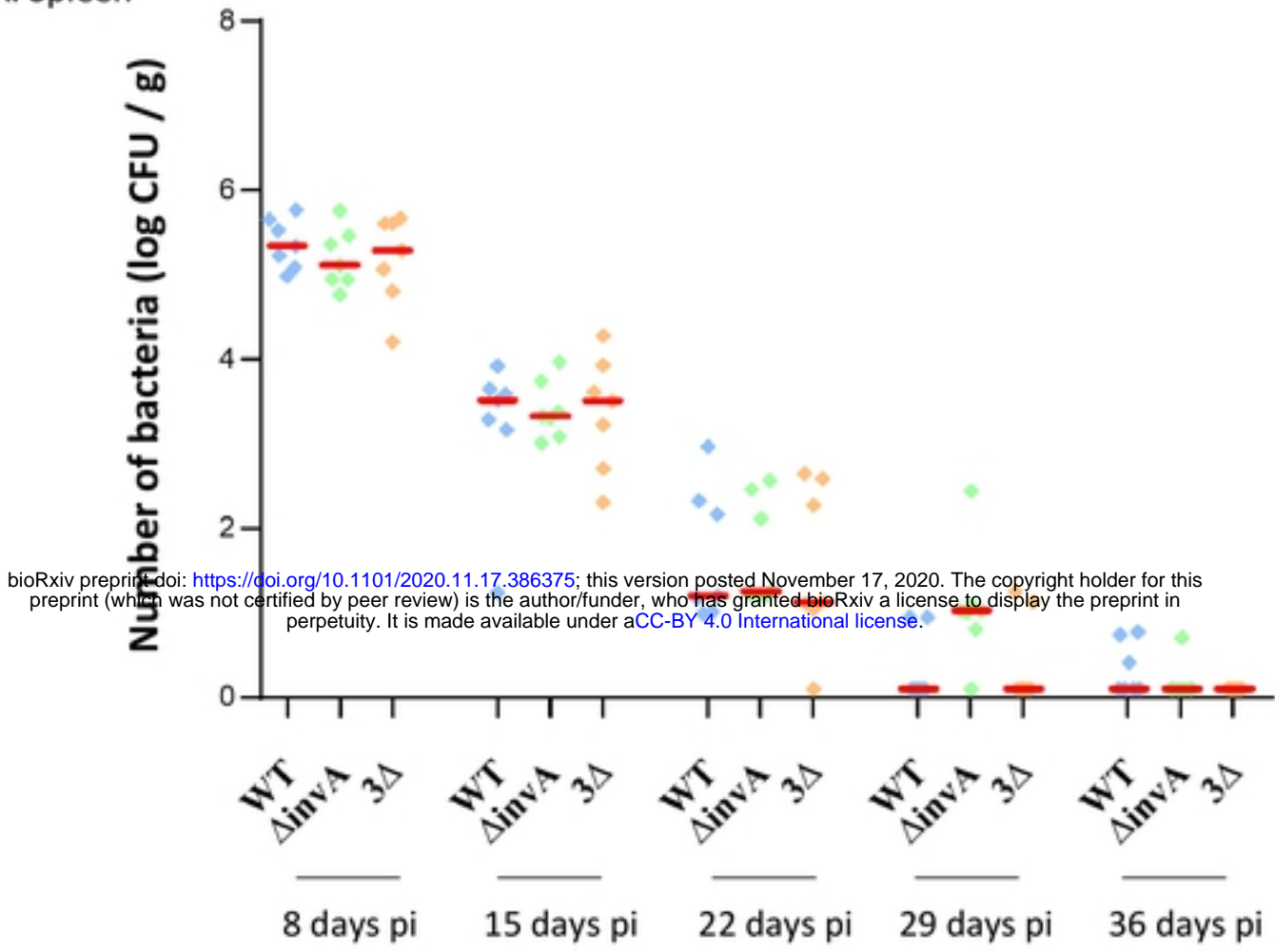


Figure 7

Fig 8. Persistence of the bacteria in the spleen and the gall bladder

A. Spleen



B. Gall bladder

